

**POLITECNICO DI MILANO**

Scuola di Ingegneria Industriale e dell'Informazione  
Corso di Laurea Magistrale in Ingegneria Biomedica



**FE Parametric Model  
(Patient Specific) of a Femur**

**Student:** Piergiorgio CANCI, 836927

**Supervisor:** *Prof. Ing.* Tomaso VILLA

**Co-supervisors:** *Dr. Ing.* Fabio GALBUSERA

*Prof. Ing.* Bernardo INNOCENTI

**Academic Year 2015-2016**

# Table of Contents

<b>1</b>	<b>ABSTRACT .....</b>	<b>4</b>
1.1	Sommario .....	4
1.2	Abstract.....	7
<b>2</b>	<b>STATE OF ART .....</b>	<b>10</b>
2.1	Hip Joint .....	10
2.1.1	Anatomy and Axes of the Hip Joint and of the Femur .....	10
2.1.2	Classification of the Pathologies of the Hip Joint .....	14
2.2	Total Hip Arthroplasty.....	16
2.2.1	Design Requirements.....	17
2.2.2	Components and Material.....	18
2.2.3	Biomechanics of Total Hip Arthroplasty.....	20
2.2.4	Failure.....	23
2.3	Typologies of Hip Prostheses .....	25
2.3.1	Femoral Level Fixation .....	26
2.3.2	Stem Design.....	33
2.3.3	Modularity .....	35
2.4	Introduction to the Finite Element Analysis .....	36
<b>3</b>	<b>AIM OF THE STUDY .....</b>	<b>38</b>
<b>4</b>	<b>MATERIALS &amp; METHODS .....</b>	<b>39</b>
4.1	FE Model Development.....	39
4.1.1	Points Acquisition.....	39
4.1.2	Geometry Realization .....	42
4.1.3	Material Realization .....	44
4.1.4	Load and Costraints Assignment.....	48
4.1.5	Mesh .....	52
4.2	Parametric Model .....	53
4.2.1	Modification of Geometry .....	53
4.2.2	User Interface .....	59
4.2.3	Prosthesis (THA) Addition – Femoral Head Excluded .....	62
4.3	Analytical Model.....	65
4.4	Output.....	68
<b>5</b>	<b>RESULTS &amp; CONCLUSION.....</b>	<b>70</b>
5.1	Geometry Adaptation of the Model.....	70
5.2	Validation of the Model.....	71

5.3	Comparison with the Gold Standard Model .....	78
5.4	General Simulation .....	84
5.5	Simulation's Speed & Number of Elements.....	87
5.6	Discussion & Conclusion .....	88
<b>6</b>	<b>FUTURE DEVELOPMENTS .....</b>	<b>92</b>
<b>7</b>	<b>BIBLIOGRAPHY.....</b>	<b>94</b>

# 1 ABSTRACT

## 1.1 Sommario

Il progetto di tesi proposto è stato svolto in collaborazione col BEAMS, un laboratorio di ricerca presso la ULB (Université Libre de Bruxelles), sotto la supervisione del Prof. Bernardo Innocenti.

L'obiettivo di tale progetto è stato quello di realizzare un modello ad elementi finiti di femore, del quale però fosse possibile modificarne la geometria, i materiali, i carichi e la dimensione della mesh. Di particolare interesse è proprio il primo parametro gestibile; in questo modo è infatti possibile ottenere geometrie di femore specifiche di un dato paziente, permettendo quindi di ricavare risultati molto più attendibili e veritieri.

Il progetto ha quindi previsto in una prima fase la realizzazione del modello di default, utilizzando opportuni file, scritti in linguaggio python, che permettessero di costruire la struttura del femore nel software Abaqus. Per poter fare ciò, sono stati utilizzati una serie di punti, ottenuti in un precedente studio, identificativi della geometria della parte corticale e spongiosa del femore. Questi sono stati ricavati da un modello sawbone; l'ottenimento delle coordinate di tale punti è avvenuto sul software SolidWorks, dove il modello 3D del sawbone in questione è stato sezionato trasversalmente da un certo numero di piani, distanziati di una certa quota l'uno rispetto l'altro, e, per ogni piano, sul contorno più esterno sono stati identificati 18 punti equidistanziati. Il modello 3D usato per poter fare ciò è stato realizzato effettuando una CT scan sul sawbone e le *slices* generate da questa sono poi state riassemblate dal software MIMICS; la struttura risultante è stata quindi importata in SolidWorks per effettuare il procedimento precedentemente descritto.

Dopo aver quindi opportunamente importato i punti in Abaqus e aver quindi generato la parte corticale e spongiosa dell'osso, questi sono stati collegati tra loro da linee, per poi definire una superficie tra di esse. Successivamente le due parti sono quindi state assemblate assieme in modo da poter ottenere il modello di femore finale. A questo sono quindi state assegnate:

- Opportune caratteristiche meccaniche, differenti, ovviamente, per le due parti,
- Specifiche condizioni di vincolo, in particolar modo un incastro a livello distale del femore, quindi a livello dei condili;
- Specifiche condizioni di carico agenti sulla struttura;

Riguardo i carichi agenti sulla struttura, questi non agiscono direttamente sulla superficie ossea bensì su di un *Reference Point* collegato alla superficie di interesse e su cui il carico viene distribuito in maniera uniforme. Tali superfici sono state opportunamente realizzate effettuando una partizione dell'elemento.

Lo step finale per la realizzazione del modello di default è quindi l'assegnazione della mesh; per lo studio in questione è stato scelto un elemento tetraedrico lineare.

Terminata quindi la realizzazione del modello di default, nella seconda fase del progetto tale modello è stato reso parametrico, andando a rendere tali gli script realizzati. L'utente è in grado di gestire le sezioni inizialmente citate attraverso l'utilizzo di una opportuna interfaccia, la quale, per ognuna di queste, permette di scegliere tra due opzioni; in particolare quest'ultimo può scegliere se proseguire con i dati di default oppure inserirli lui stesso manualmente.

Nel caso di inserimento manuale dei dati, questi variano in funzione della sezione di lavoro in cui ci si trova; le sezioni sono quattro e sono riportate di seguito:

- *Geometria*: permette di modificare la geometria della struttura richiedendo in input sei parametri geometrici misurabili direttamente sulle radiografie del paziente in analisi;
- *Materiali*: richiede prima di scegliere tra un comportamento isotropo o trasversalmente ortotropo del materiale e successivamente è necessario definire, in funzione della scelta, modulo di Young, coefficiente di Poisson e modulo di taglio, se trasversalmente ortotropo, o modulo di Young e coefficiente di Poisson, se isotropo;
- *Carichi*: richiede l'inserimento delle tre componenti, nelle rispettive tre direzioni principali, della forza che si vuole utilizzare. I valori delle forze muscolari non sono invece gestibili;
- *Mesh*: permette di definire l'*Element Size* con cui si vuole discretizzare il dominio del modello.

Ulteriore possibilità concessa all'utente è infine quella di applicare o meno una protesi al modello; nel caso dell'applicazione l'utente può scegliere tra applicare una protesi in Ti6Al4V, CoCrMo o definendo le caratteristiche meccaniche della stessa.

In modo da poter verificare il funzionamento del modello, è stata effettuata prima di tutto una verifica dell'adattamento geometrico del modello a differenti profili femorali. Per poter fare ciò sono state utilizzate due immagini radiografiche di due differenti pazienti da cui sono stati misurati i parametri di interesse richiesti dall'interfaccia; il modello ad elementi finiti derivatone è stato poi confrontato otticamente con l'immagine radiografica di partenza.

Successivamente, la vera e propria validazione dell'accuratezza e precisione dei risultati, è stata eseguita confrontando il modello parametrico con un uno analitico opportunamente realizzato e su cui vigono le ipotesi di De Saint Venant. Il confronto è stato compiuto usando gli sforzi massimi, per la zona in trazione, e minimi, per quella in compressione, misurati da Abaqus sull'osso sul modello ad elementi finiti con quelli calcolati manualmente sul modello analitico. La scelta dell'utilizzo degli sforzi massimi e minimi principali non è casuale bensì legata al comportamento fragile dell'osso.

Non essendo poi stata utilizzata, nel caso di applicazione della protesi, una interazione tra superfici totalmente appropriata e che rispecchiasse quella fisiologica, è stato inoltre necessario valutare quanto i risultati differissero rispetto ad un modello che prevedesse un tipo di interazione più corretta; per questa ragione è stato quindi utilizzato un modello Gold Standard, con cui si potesse effettuare un confronto in termini di sforzi registrati sia sulla componente protesica che ossea. Per fare ciò sono state utilizzate le sette ROI di Gruen, sei per la protesi in quanto la ROI 4 include unicamente la componente ossea e quindi non compare. Per la componente protesica sono stati misurati ed utilizzati gli sforzi di Von Mises, per via del comportamento duttile dell'impianto, mentre per quella ossea gli sforzi massimi e minimi principali.

Sono state poi confrontate le distribuzioni di sforzi massimi e minimi principali a livello osse nelle ROI di Gruen in presenza di un femore sano, quindi senza nessuna protesi applicata, con protesi in Ti6Al4V e CoCrMo. Similmente sono state valutate le distribuzioni delle deformazioni in presenza di osso fisiologico, osteoporotico ed osteopenico.

Infine è stato valutato quanto, al variare dell'*Element Size*, si modificassero i tempi di simulazione e il numero di elementi generati.

Tutti i risultati sono stati opportunamente discussi e le approssimazioni considerate nello studio, principalmente di natura geometrica, dimostrate essere veritiere e quindi corrette.

Alcuni possibili sviluppi futuri sono stati suggeriti, tra cui il più significativo è sicuramente l'estensione della parametrizzazione anche alla componente protesica oltre che femorale, dando una linea guida su quali possano essere i parametri di modifica, e quali possano essere le criticità legate a questo tipo di implementazione.

## 1.2 Abstract

The following thesis project has been developed in collaboration with the BEAMS department at the ULB (Université Libre de Bruxelles), under the supervision of Prof. Bernardo Innocenti.

The aim of the project has been to realize a FE model of the femur, which geometry, materials, loads and element size of the mesh are manageable and modifiable. Relevant aspect is in particular the first parameter manageable; indeed, in this way it is possible to obtain femoral geometry specific of a datum patient, allowing to achieve results much more reliable and correct.

In the first part of the study the default model has been realized, by using appropriate scripts written in Python language, which allowed to realize the femoral structure on the software Abaqus. In order to accomplish this, a series of points have been used, obtained in a previously study, identifying the geometry of the cortical and spongious part of the femur. Their coordinates have been calculated starting from a sawbone model of the limb; the achievement of the above-mentioned coordinates has been conducted on the software SolidWorks, where the 3D model of the sawbone has been cutten by using a certain number of transversal planes, separated one to the other by a certain distance. For eache plane 18 equispaced points have been identified on the outer profile. The 3D model used to do that has been realized by applying a CT scan to the sawbone and the *slices* obtained have been then reassembled by using the software MIMICS; the resultant structure has been imported in SolidWorks to proceed with the process just described.

After having properly imported the points in Abaqus, those laying on the same plane have been connected by using the *Wire* function, recreating in that way the outer profile of the two part of the femur, the cortical and spongious one. After applying a surface between the different wires the two parts have been then assembled together to obtain the conclusive shape of the femur. To this one have been then assigned:

- Properly mechanical properties, obviously different for the two parts;
- A specific boundary condition, in particular an encastre at the distal level of the femur, which means at the level of the condyles;
- Loads acting on the structure;

Regarding the loads, those do not directly act on the bone surface but rather on *Reference Points* which are connected to the surface of interest and distribute the load uniformly on them. Those surfaces have been properly realized by partitioning the model.

The final step of the procedure to realize the default model has been the assignment of the mesh; for this work a solid linear tetrahedral one has been chosen.

Completed the realization of the default model, in the next step of the project, the model has been made parametric, by properly modifying the scripts realized. The user can manage the sections initially mentioned by using an easily usable interface and, for each one of these, this one allows to choose between two main options; in particular the user can choose to proceed with the default data or to manually define them.

In case of manually insertion of the data, these vary in function of the job section; those are the following:

- *Geometry*: allows to modify the geometry of the default model and, in order to do that, requests six different parameters directly and easily measurable on the radiographic image of the patient;
- *Materials*: requests first to choose the mechanical behaviour of the material (isotropic or transversal orthotropic) and then depending on the answer of the user, it is requested to type the Young Modulus and the Poisson Coefficient, if isotropic properties have been chosen, or the Young Modulus in the three directions, as well for the Poisson Coefficient and the Shear Modulus, if transversal orthotropic properties have been chosen;
- *Loads*: requests to type the three components of the force acting on the femoral head along the three main direction. On the contrary, the muscular forces are not manageable;
- *Mesh*: allows to define the *Element Size* which is going to be used to mesh the model.

An additional possibility given to the user is to choose between applying or not a prosthesis to the model; in case of application the user can decide between applying a Ti6Al4V, CoCrMo prosthesis or by defining its mechanical properties.

In order to confirm whether this job properly responds to the adaptation to different femoral shapes, two radiography have been used from which the parameters of interest requested by the interface have been measured; the FE model realized by using them has been then optically compared with the starting x-ray image

Subsequently, the real validation of the accuracy and precision of the results, has been achieved by comparing the ones of the parametric model with the ones calculated on an analytical model properly realized, by using the Saint Venant hypothesis. The comparison has been fulfilled by using the maximum, on the area subjected to traction, and minimum, on the area subjected to compression,



principal stresses, measured from Abaqus on the bone on the FE model with the one manually calculated on the analytical model. The reason why the maximum and minimum principal stresses have been used is a consequence of the fragile mechanical behaviour of the bone, which do not allow the use of the Von Mises stresses.

It has been also important to validate the model with the prosthesis applied, since the interaction between the prosthesis and the bone in the parametric model has been approximated with a function which doesn't completely represents the physiological case; in order to evaluate the differences or error induce by this one, a Gold Standard model has been introduced, where a more appropriate interaction has been used. To fulfill the comparison, either on the prosthetic and bone component, have been identified the ROI of Gruen, seven for the bone and six for the prosthesis, where the maximum stresses have been calculated. Those are in terms of Von Mises stresses for the prosthetic part, due to the ductile behaviour of the prosthesis, and maximum and minimum principal stresses on the bone.

Moreover, maximum and minimum principal stresses distribution have been measured on the bone, in the ROI of Gruen, and compared in presence of a healthy femur, which means without prosthesis, Ti6Al4V and CoCrMo implant. With a similar process, the strain distribution in presence of a healthy, osteoporotic and osteopenic femur has been also evaluated.

Lastly, it has been calculated the variation of the simulation's speed and number of elements generated on the model by modifying the *Element Size*.

All the results have been properly discussed and the approximations introduced in the study, mostly regarding the geometrical part, have proved to be admissible and correct.

Some possible future developments have been suggested; the most relevant is regarding the extension to the parametrization also to the prosthetic component. Some guide lines have been suggested to fulfill this task, about the parameters that could be used to parametrize it, and which could be the most important criticalities on this kind of implementation.

## 2 STATE OF ART

### 2.1 Hip Joint

#### 2.1.1 Anatomy and Axes of the Hip Joint and of the Femur

The hip joint (Figure 1), also known as coxo-femoral joint, is a typical ball and socket joint. This notation implies joint's mobility, spherical or hemispheric shape of the articular surfaces and the presence of a spherical concavity. The main components are the acetabulum, a hemispheric articular cavity, and the femoral head, corresponding to  $2/3$  of a sphere with a diameter of 4-5 cm. The connection between those two is guaranteed by the presence of the acetabulum labrum, providing a spherical coupling.

Moreover, either the acetabulum and the femoral head are covered by a cartilage layer the main purpose of which is to absorb impacts and to guarantee a correct movement between those two surfaces, thanks to the additional presence of the synovial fluid [1].

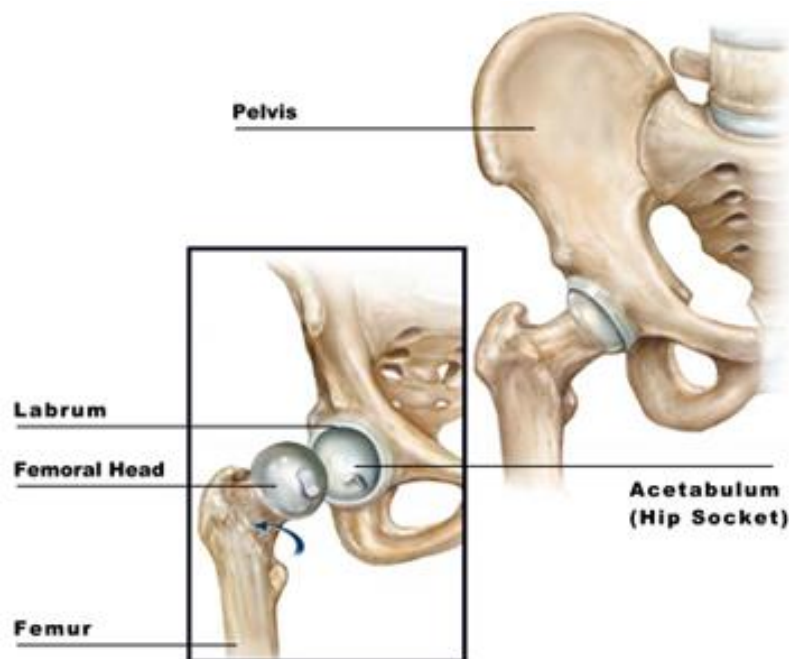


Figure 1: Hip Joint's Anatomy [16].

The loads acting on the hip joint are the highest in the human body; indeed, it is enough to think that during the bipodalic stance [2] the 62% of the body weight, excluding the lower limbs, is acting on the two joints.

However this consideration is not correct during monopodalic stance. Considering just the static case, the resultant load on the hip joint is dependent on three main parameters:

- The weight of the lifted limb, corresponding to 19% of the body weight;
- The movement of the center of gravity;
- The weight of the trunk.

So, during walking the hip joint is subjected to a resultant force given by the cross product between the body weight and the moment generated by the contraction of the abductor muscle, in the amount of 5-7 times the body weight (Figure 2); those can represent a cause of failure, either of a healthy joint or of a prosthesis.

activity	max. joint force		angular velocity at max. load		stance phase flexion range			
	body weight		rad/s		degrees			
	hip	knee	hip	knee	hip		knee	
level walking								
slow	4.9	2.7	0	0.6	-19	26	9	57
normal	4.9	2.8	0	1.4	-11	31	5	71
fast	7.6	4.3	0	3.7	-12	36	2	72
up stair	7.2	4.4	0.8	0.8	-1	37	20	67
down stair	7.1	4.9	0.3	1.2	12	30	18	87
up ramp	5.9	3.7	0.1	0	-12	30	18	47
down ramp	5.1	4.4	1.7	2.3	-11	25	18	37

*Figure 2: Joint Load's Values, Range of Angulation and Angular Velocity for Different Activities [2].*

The effect of the resultant force on the femoral neck is strictly dependent on the CCD (Centrum Collum Diaphyseal Angle), which represents the angle between the femoral diaphysis and neck.

Anatomical anomalies like cases of varus and valgum deformity imply variation of the CCD. For example, in presence of valgum deformity, higher forces from the abductor muscle are required to preserve equilibrium; the direct consequence is that the resultant force on the hip joint increases too.

Regarding the femoral axis [10], this one is not exactly perpendicular to the ground. A mechanical and an anatomical axes can be distinguished:

- The mechanical axis is obtained by drawing a line connecting the center of the femoral head and the center of the ankle joint, which corresponds to an approximately 3° slope compared with that of the vertical axis (Figure 3);
- The anatomical axis can be obtained in two different ways. The first method consists in drawing a line into the intramedullary canal, whereas the second consists in taking two points in the femoral shaft, where the first one is placed 10 cm above the knee joint and both of them are located at an equal distance between the medial and lateral cortex (Figure 3).

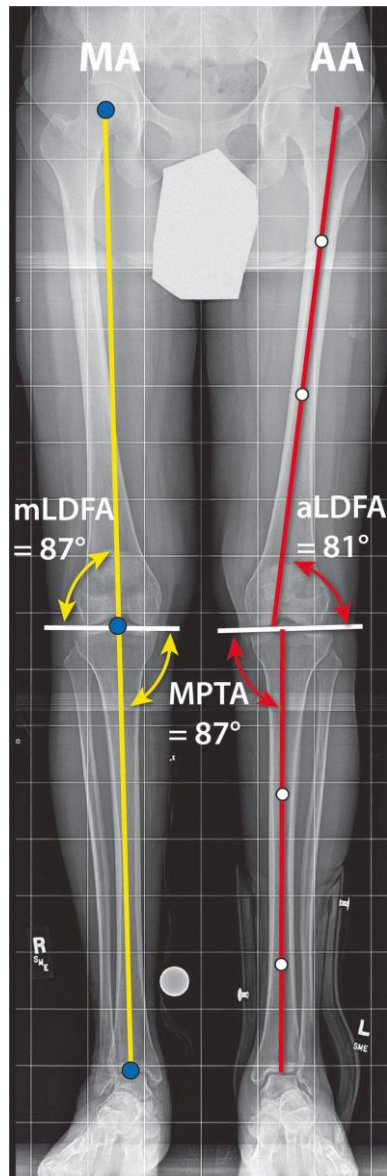


*Figure 3: Representation of the mechanical (MA, yellow) and anatomic (AA, red) femoral axis in the plane between the condyles and the femoral head; are also showed the mechanical lateral distal femoral angle (mLDFA), anatomic lateral distal femoral angle (aLDFA) and medial proximal tibial angle (MPTA) [10].*

In a healthy patients the average angle between the femoral axis and the knee joint axis, which is the one that connects the two extremities of the condyles and it is represented in Figure 3 with a white line, is 87° and 81°, mechanical and anatomical respectively.

### 2.1.2 Classification of the Pathologies of the Hip Joint

The pathologies [4] that can affect the hip joint can be classified as follows:

- Degenerative;
- Inflammatory;
- Congenital anomalies;
- Trauma.

*Degenerative Processes* are typically characterized by arthrosis (Figure 4), that implies the degeneration of the cartilaginous layer with a reduction of its thickness. It can be distinguished in primary or secondary arthrosis; the main difference between these two is that the second one is a consequence of trauma, structural pathologies (e.g. osteoporosis) or inflammation that produce wear at the joint level while the first one is a direct degeneration of the cartilaginous layer which can also causes direct osseous contact [17].

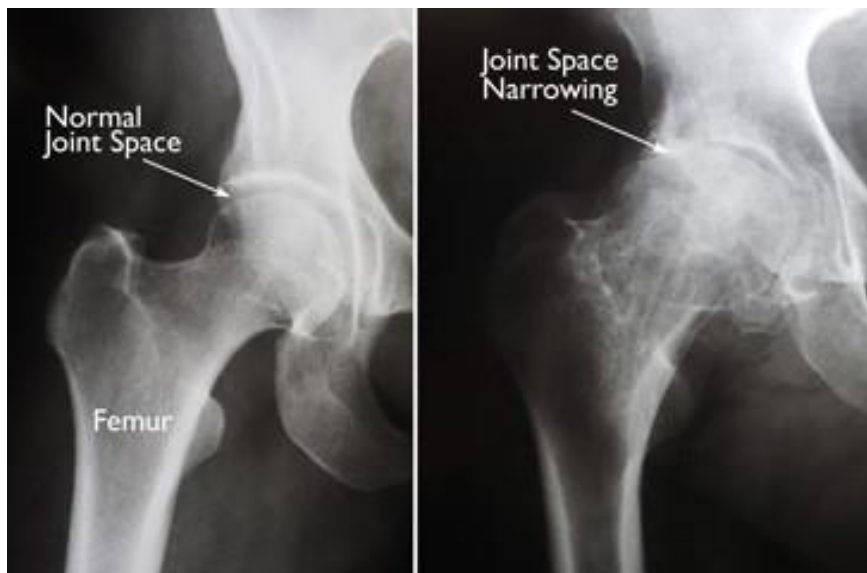


*Figure 4: Hip arthrosis (right) implies loss of the cartilagineous layer and consequently a reduction of the joint space respect the healthy condition (left) [18].*

A typical example of an *Inflammatory Process* is the rheumatoid arthritis which implies intense pain due to an inflammation of the synovial fluid. In this case it is usually possible to maintain the acetabulum side while it is necessary to replace the femur's head [19].

*Congenital Anomalies* derive from genetic anomalies; an example is the hip dysplasia (Figure 5) during which the femoral head gradually dislocate from the acetabulum cavity due to a non-physiological translation of the first one in the second one. Another typical example is the congenital hip luxation; the effects are similar to hip dysplasia but in this case the dislocation is a consequence of a non-physiological dimension of the acetabulum [20].



*Figure 5: Hip dysplasia (on the left) [42].*

The last two typical anomalies are the coxa valga and vara; the parameter subjected to modification is the CCD that in a healthy patient is around  $120^{\circ}$ - $135^{\circ}$  while in presence of coxa valga is higher than  $135^{\circ}$  and of coxa vara is less than  $120^{\circ}$  (Figure 6).

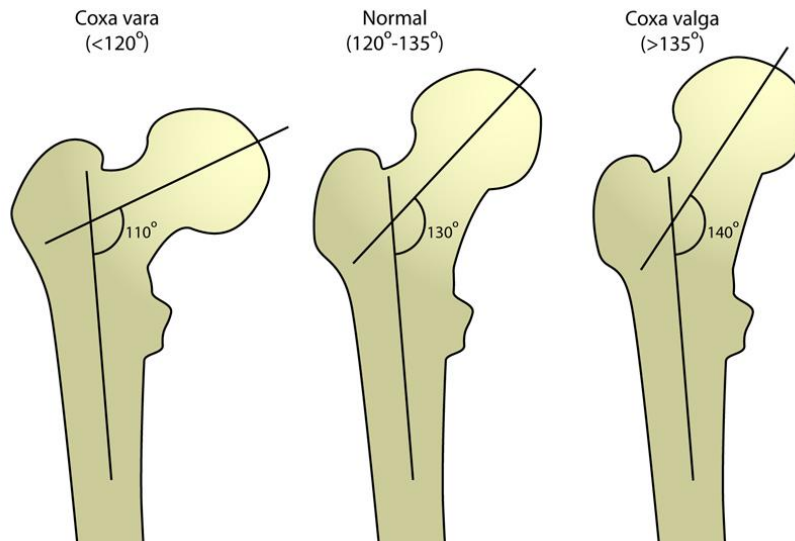


*Figure 6: Representation of the CCD for a patient subjected to coxa vara, valga and for an healthy patient.*

Typical *Traumatic Pathologies* are traumatic hip luxation, acetabular fracture, femoral epiphysis fracture, complications from fractures; depending on their level of criticality the implantation of a prosthesis could be required or not. On the contrary, osteonecrosis represents a situation in which prostheses are commonly implanted. It entails an insufficient femoral head's blood perfusion followed by necrosis of its bone tissue. Moreover, patients suffering osteoporosis are most inclined to fractures following trauma, since the bones result already debilitated [21]. In most of the case it is necessary the substitution with an hip joint prosthesis.

## **2.2 Total Hip Arthroplasty**

Total Hip Arthroplasty (THA) is a surgical intervention with the purpose to restore the hip joint's functionality; during the surgery either the acetabular cavity and the femoral head and neck are removed and replaced with the prosthesis components. Final objective of the procedure is to achieve an articular and mechanical stability, which is guaranteed by physiologically sollecitating the biological structure. Indeed, an excessive sollecitation of the bone component can entails fractures and consequently osteonecrosis, while on the contrary a non sufficient sollecitation implicates bone resorption [22].



A THA is mostly required [41] when in presence of the following hip diseases:

- *Osteoarthritis*: it is an age-related "wear and tear" type of arthritis and it usually shows up in people over 50 years of age and, often, in individuals with a family history of arthritis. This disease implies that the cartilage cushioning the bones of the hip wears away; consequently, the bones rub against each other, causing hip pain and stiffness. Osteoarthritis may also be caused or accelerated by irregularities in how the hip developed in childhood;
- *Rheumatoid arthritis*: The synovial membrane becomes inflamed and thickened. As a consequence the inflammation process can damage the cartilage, involving pain and stiffness (Ref "2.1.2 Classification of the Pathologies of the Hip Joint");
- *Post-traumatic arthritis*: It can be a consequence of an hip injury or fracture. The cartilage may become damaged and involve hip pain and stiffness;
- *Avascular necrosis*: Injuries to the hip, like a dislocation or fracture, may limit the blood perfusion to the femoral head; this process is known as avascular necrosis (also commonly referred to as *osteonecrosis*). The lack of blood may cause the surface of the bone to collapse, and arthritis will result;
- *Childhood hip disease*: Even though those disease are successfully treated during childhood, they may still cause of arthritis later on in life, due to a non-physiological growth of the joint.

### 2.2.1 Design Requirements

The following requirements [4] are strictly necessary:

- To allow degrees of freedom between the leg and the pelvis as similar as possible to the physiological ones. That is the reason why the shape of the prosthesis is very similar to the one of the physiological joint;
- To guarantee reliability of the device; in particolare during the development it is important to consider that the loads acting could be even a couple of times higher than the Body Weight (BW). In some scenarios [5] loads in the amount of 4 times the BW were observed during walking, or even 11 times during accidental stumble;
- Sufficient fatigue loading resistance. The prosthesis life expectancy is around 10 years [ref – penso che attualmente ci si possa aspettare di più]; taking in count a number of steps of 1

million/year, the prosthesis has to resist for 10 million cycles. In particular the component which is more subjected to fatigue loading is the stem;

- The joint's surfaces have to resist wear, or at least this one should not influence the prosthesis' functionality and the biocompatibility with the neighbouring tissues.
- The materials used have to guarantee biocompatibility, that means no alterations or undesired responses from the tissues have to occur, but at the same time they should be able to interact with them in order to obtain mechanical stability;
- The prosthesis should be easily implantable and replaceable in case of malfunctionality or damage to one of its component. For this reason it is necessary to preserve as much as possible bone tissue during the implantation.

### 2.2.2 Components and Material

The main components [4] of a hip prosthesis are shown in Figure 7:

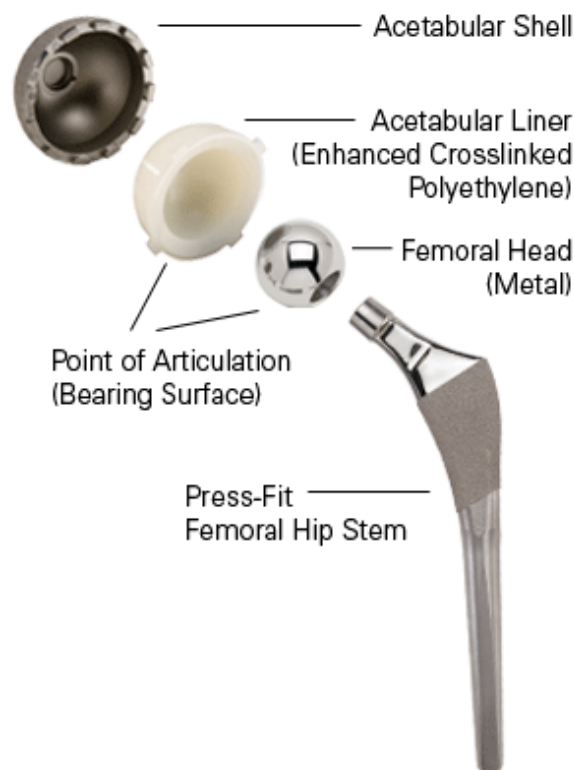


*Figure 7: Main components of a hip prosthesis [43].*

The materials chosen are the following:

- For the Femoral Hip Stem  $Ti_6Al_4V$  is usually used (Young's modulus = 110 GPa,  $\sigma_y = 700-800$  MPa) or alternatively Cr-Co\_Mo (Young's modulus = 220 GPa,  $\sigma_y = 1000$  MPa) or stainless steel AISI 316 L (Young's modulus = 210 GPa,  $\sigma_y = 800$  MPa). All these materials have high biocompatibility, mechanical properties and wear resistance. The reason why  $Ti_6Al_4V$  is the most used is because it incentivizes the most osseointegration, by stimulating the production of ECM and proteins [23].

Osseintegration can be improved by covering the stem with [8]:

- a porous steel (sphere or microsphere);
- hydroxyapatite or bioglasses;
- PMMA.

Regarding the surface finishing process, the most common are polishing and sandblasting;

- The Acetabular Shell, also known as metal back is usually made of  $Ti_6Al_4V$ . Sometimes is coupled with screws to guarantee a major mechanical stability (Figure 8);

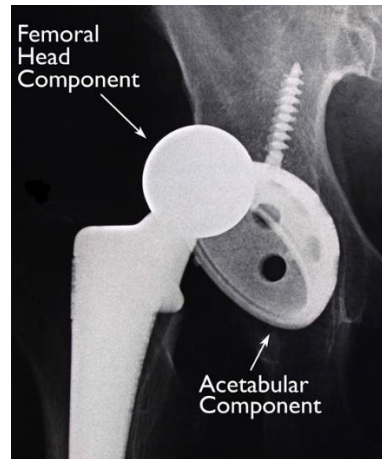


*Figure 8: Connection of the acetabular shell to the bone with a screw.*

- The Femoral Head-Acetabular Liner coupling can be of different kind:
  - CoCr alloy/UHMWPE;
  - Alluminia/Alluminia;
  - CoCr alloy/CoCr alloy.

The most used is the first one; even though this coupling releases a high amount of debris, under a certain threshold quantity it can be digested by physiological processes (*Ref. “2.2.4 Failure”*).

The second coupling is very advantageous with respect to the release of debris but at the same time in case of sudden impacts it can face breakages.

The third one is very convenient either for the amount of particles and for mechanical properties. However, even though the quantity of debris released is very low those are highly toxic to the organism (they induce metallosis); this is the reason why this kind of coupling is not pretty much used anymore [24].

## **2.2.3 Biomechanics of Total Hip Arthroplasty**

### **2.2.3.1 Range of Motion (RoM)**

The Range of Motion [5] is a parameter that allows defining the joint mobility and represents the maximum excursus that a body component can cover from a start point to a finish one. After the implantation of the hip prosthesis, the joint mobility is subjected to modifications; these are strictly dependent on the prosthesis design, in particular the size of the femoral head and its position in the acetabulum have a central role.

The femoral head diameter ( $\Phi$ ) varies from 22.25 mm to 60 mm; the following classes can be identified:

- Small:  $22 < \Phi < 28$  mm;
- Medium:  $28 < \Phi < 36$  mm;
- Large:  $36 < \Phi < 60$  mm.

Moreover, in some cases femoral heads are patient-specific, thus having the same dimension of the patient's physiological femoral head.

As said earlier, the femoral head dimension directly influences variation of RoM; indeed, considering a 28 mm and a 36 mm there is a gap of  $13^\circ$  (from  $123^\circ$  to  $136^\circ$ ) [5]. Moreover, by using a larger femoral head, the jumping distance (Figure 9), which represents the distance the head has to “jump”

before leaving the cup (Cit. Morlock et al., *Biomechanics of Hip Arthroplasty*, 2011), increases too; this parameter the higher is, the better is because the prospect of dislocation will be reduced.

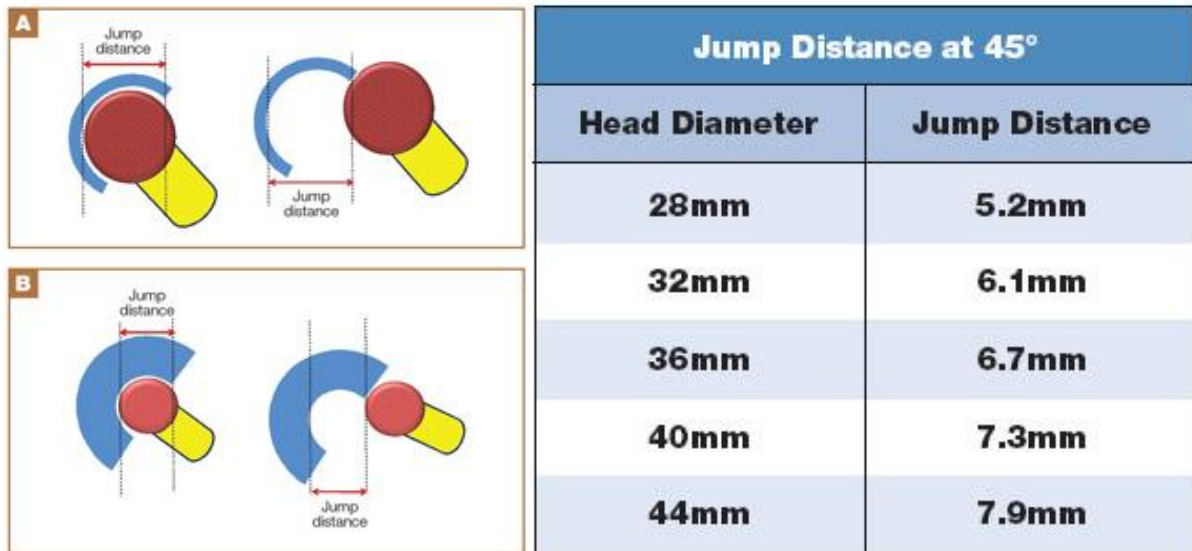


Figure 9: Relation between jump distance and head diameter [26].

The second main design aspect that influence the RoM is the cup entrance plane. This one can be hemispherical or sub-hemispherical, in which the only difference lies in the dimension of the expansion angle of the acetabular cup; indeed, in the first case this one is around 180°, while in the second one the angle is smaller (around 152-160°). That implies the center of rotation of the femoral head is outside the acetabular cup area, allowing wider range of movements of the taper before getting obstructed by the cup (Figure 10).

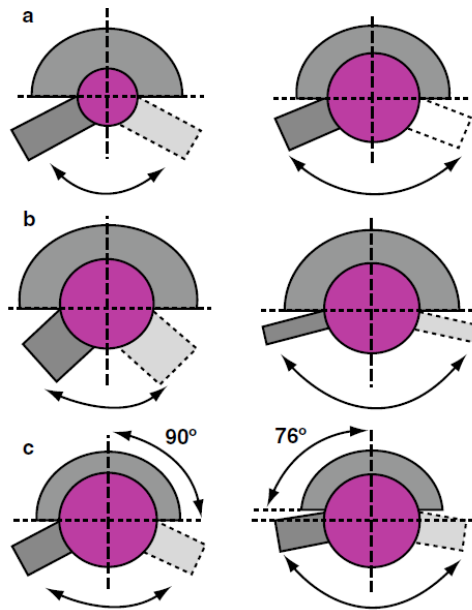


Figure 10: RoM influenced by femoral head dimension (a), taper diameter(b), hemispherical/sub-hemispherical (c) [5].

However, using large heads implicates two main disadvantages [25]:

- The friction increases with head diameter entailing possibility of cup loosening and taper corrosion;
- The forces to relocate the joint, due to the friction, increase with larger heads.

In conclusion, a 36 mm head is usually used, since represents a good balance between the advantages and disadvantages.

### 2.2.3.2 Tissue Damage and Joint Tensioning

The stability of the hip joint is also influenced by the amount of soft tissue damaged during the surgery and the tension in the remaining soft tissue after THA implantation. Both the surgical technique and the experience of the surgeon assume a very important role in this field; indeed, assuming that the first one is the same, the surgeon determines the extent of the involvement of the soft tissue structures and the positioning of the implant.

During the operation, damages to hard tissue could occur, with consequences like fractures or fissures of the bone, or even micro fractures in the trabecular bone, that could evolve potentially in fractures [5].

For what concern an eventually loosening of tension of the soft tissue, this can determine hip subluxation. In this case the formation of a properly scar tissue which will have to possess either elasticity is very important, in order to guarantee movement, or the capability to assure stability to the implant.

#### **2.2.4 Failure**

Failures can occur at different times after implantation. That is why instead of classifying them based on their typology they are distinguished as follows [4]:

- Short Term Failures:
  - Septic loosening is caused by infection; in case this is limited to a small area around the prosthesis, it is sufficient to remove this one and replace it with a new one. But if the infection interests a wider area it will be necessary to apply spacers; those devices are typically made in the same material as bone cement and contain pharmacological substances to reduce the inflammatory response and the infection. The spacers are temporary and their shape is similar to the prosthesis that will be implanted, so they conserve both physiological spaces and dimensions;
  - Recurrent dislocation is mostly a consequence of an incorrect surgical positioning. In most cases the interested area is the acetabulum, so it is sufficient to modify the acetabular compartment or, in presence of modular prosthesis, the femoral head;
  - Intolerance (allergy) to one of the components material. The only way to solve this problem is to remove the current prosthesis and apply a new one, after the identification of the material which has started the allergic response.
- Medium Term Failures:
  - Structural failure, which is caused by an inadequate sollecitation of the bone tissue;
  - Aseptic mobilization has as a consequence the loosening of the prosthesis grip into the bone and it is not caused by an infective process. Physiologically a progressive reabsorption of the bone around the prosthesis can be observed, with a consequent

genesis of cavities (periprosthetic osteolysis). This kind of failure can be induced by two different mechanisms. The first one is when the bone tissue is not sufficiently mechanically stimulated, so it starts to reabsorb causing mobilization of the implant. On the other hand, if the prosthesis implanted is a cement one, the failure can be caused by a yielding of the cement's mantle.

- Long Term Failures:

- Fatigue structural failure of a component of the prosthesis due to an high number of sollecitations;
- Aseptic mobilization due to debris periprosthetic osteolysis represents one of the most recurring causes of long term failures. It implies a decrease of the bone tissue in the area around the prosthesis. A study [6] reports that the greater trochanter is the most subjected to this phenomenon (Figure 11).

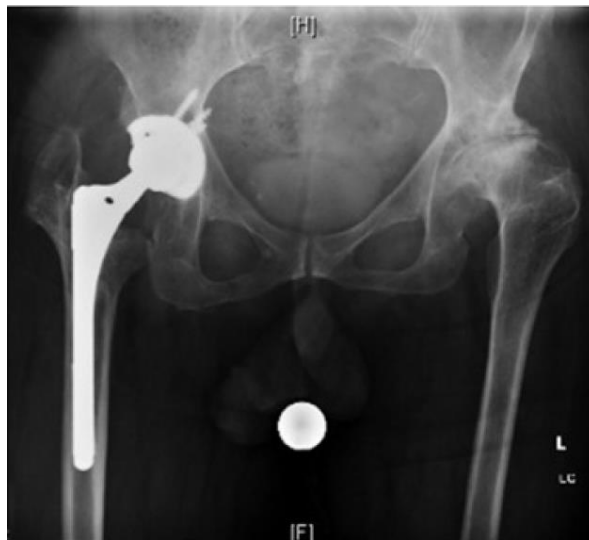


*Figure 11: Reduction of bone tissue around the prosthesis area, either at the level of the greater and lesser trochanter.*

The particles that induce periprosthetic osteolysis originate from two main processes: wear and corrosion. In the first case the one that produces most debris is the one that has place between the femoral head and the acetabular liner, known as abrasive wear; moreover, this process can be incentivized by the third-body wear, whose foreign particles derive from the cement (if it is a cement prosthesis) or bone residuals of the surgical intervention [27]. Seeing as how UHMWPE is the most subjected to abrasive wear, it is important to evaluate an estimate of particles before the implant, since PE's



fragments over a certain threshold can generate a foreign body response. Therefore a few methods exist , to accomplish that, using a physiological mixture (water and salt) to emulate biological conditions:

- Physically gathering of the debris produced during the test;
- Weighing the sample before and after the test. The main problem is that the UHMWPE absorbs part of the solution during the test so this one will increase his effective weight;
- Scanning the sample before and after the test. It is basically used an optical evaluation of the volume's variation. In this case the test's weakness is linked to the mechanical nature of the polymer; the surface's alterations are not caused just by the wear but also by the cyclic loading applied. So it is important to evaluate the mechanical response of the sample during static loading (creep) and therefore proceed with the test.

The other typologies of wear (adhesive, corrosive, erosive and fatigue wear) do not influence so much the debris release in the THA [7].

Regarding the corrosion, this has place on metallic surfaces and entails releasing of metallic ions.

### **2.3 Typologies of Hip Prostheses**

Hip prostheses can be classified in different ways.

It is possible to classify them in function of the percentage of bone removed:

- Endoprosthesis: the substitution interests only the femoral component while the acetabular part is kept physiological;
- Total Hip Arthroplasty (THA): either the femoral and acetabular part are substituted with the prosthesis (Figure 12);
- Resurfacing: similar to the THA but either the physiological femoral neck and body are preserved. It is mostly applied in young patients, when the case allows, in order to have available bone tissue for new potential implants (Figure 12) [4].

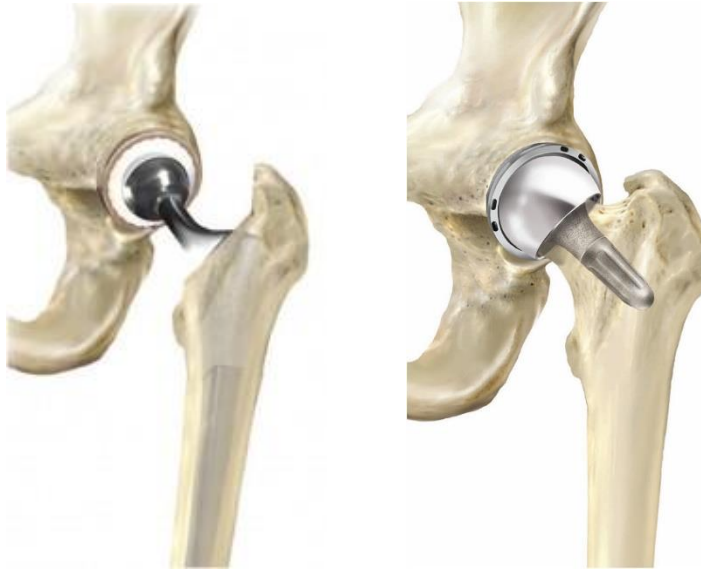


*Figure 12: THA (on the left) and Hip Resurfacing (on the right) [28].*

They can be also classified according to the method used to guarantee their fixation to the bone (cemented or cementless), the length of the stem and their modularity.

### **2.3.1 Femoral Level Fixation**

#### **2.3.1.1 Cement Fixation**

In this kind of prosthesis, the cement is introduced in the gap between the stem and the bone tissue (Figure 13).

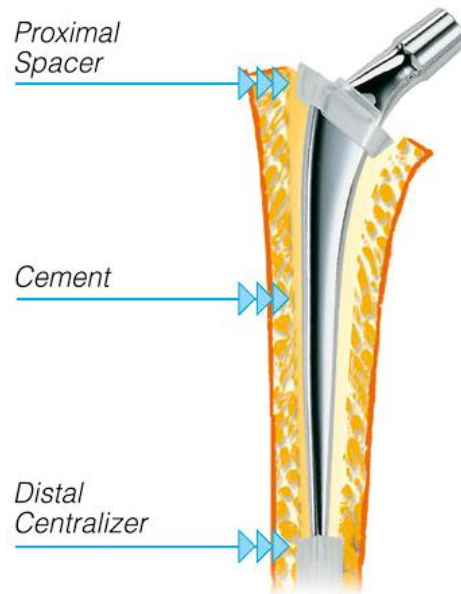


*Figure 13: Cement prosthesis.*

Its mechanical purpose is to guarantee a mechanical primary stability and to spread the shear and compression stress acting on the prosthesis to the bone tissue, to keep it continuously stimulated. It is obtained [8] in the operating room by combining a liquid constituent with a solid one, immediately before injecting it to the patient.

The solid part is made of:

- PMMA;
- Polymerization initiator: benzoyl peroxide (BPO);
- Potential additives: antibiotics, radiopaque substances.

The components of the liquid phase are:

- Monomer: MMA, MA, n-butylMA;
- Polymerization inhibitor: Hydrochinon. It is necessary to avoid polymerization before the effective use;
- Polymerization catalyst: DMPT, aromatic amine.

By using a different ratio of the two phases it is possible to modify the cement viscosity; the commonly used ratio for the hip prosthesis is around 2:1 (solid/liquid phase).

The advantages of using cement stem are [29]:

- The components dimensioning does not represent a criticality anymore thanks to the presence of the cement that links the prosthesis stem to the bone tissue;
- The surgery is simpler for the surgeon;
- a higher primary mechanical stability is guaranteed.

However there are a few disadvantages too [29]:

- The polymerization is exothermic (termic range [9] between 43° to 53°, with peak during the implant of 70°) so it is important to reduce as much as possible the thickness of the cement mantle and eventually use a higher quantity of the solid respect the liquid phase in order to reduce the amount of generated heat;
- The quantity of bone tissue removed is higher than the one of the cementless stem (Figure 14). This is a critical point when it will be possibly necessary to apply a new prosthesis.

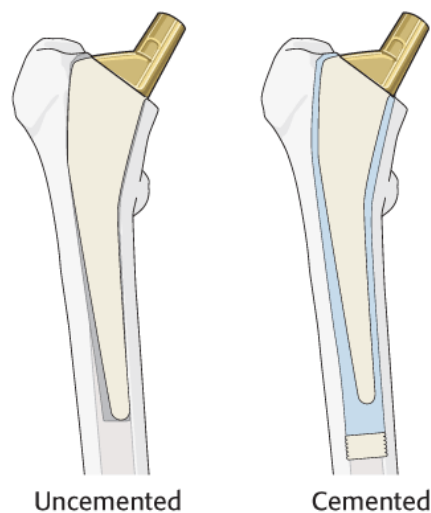


*Figure 14: Comparison between cement and cementless prosthesis in term of bone tissue removed [12].*

- Even though the cement guarantees a mechanical stability and a good fixation, this could become disadvantageous during revision. Actually, as long as the prosthesis neck is not the one which got broken, this problem can be solved by using modular prostheses;
- It is very important to remove all the cement's redundancy since potential particles residuals could start third-body wear;

- Some of the components used are toxic, so they could cause allergic response;
- After the polymerization process the cement became porous and this implies the introduction of discontinuity points, so a reduction of the mechanical properties. In order to avoid that as much as possible is important to use low cement thickness and a slow mixture procedure.

### **2.3.1.2 Cementless fixation**

In this case [4] the fixation of the stem is guaranteed by an interference fit, that means the stem is a little bit larger than the medullary cavity; that is the reason why this kind of application is also known as press fit.

The advantages are:

- Less invasivity than the cement stem. Moreover a higher quantity of bone tissue is preserved, thus easing revision;
- Since the stem is fitted into the femur there are less movement risks [4].

On the contrary, the disadvantages are:

- The surgery is more difficult than the one for the cement stem, since the surgeon has to pay a lot of attention either during the dimensioning of the medullary cavity or during the fitting of the stem;
- More care about the sizing and materials choice is required.

The stability of the stem is guaranteed by osseointegration between the bone tissue and the stem's surface. This process is induced by a fracture and a breakage of the periosteal and endosteal blood vessels, which bring the genesis of mesenchymal tissue [29]. This tissue will start to evolve in fibrous bone that is a primitive kind of bone tissue with a low mineral density, no collagen fiber's specific orientation and it result to be more elastic. In the following two months, this one will start to mineralize and calcify bringing the formation of a grown bone. During the third month the bone will be remodeled by the osteoclasts activity; the process can last either a week or a month.

In conclusion three major phases of the osteointegration process can be identified:

- Fibrous bone formation;

- Developing of a grown bone tissue;
- Remolding of the bone tissue.

In order to use this type of prosthesis, it is important to evaluate the quality and the condition of the bone; for this purpose two main indexes are commonly used [30]. The first one is Singh Index (S.I.) which express the level of bone osteoporosis using a numeration system (Figure 15), where S.I equal to 1 refers to a bone critically osteoporotic, while 6 refers to an healthy one.

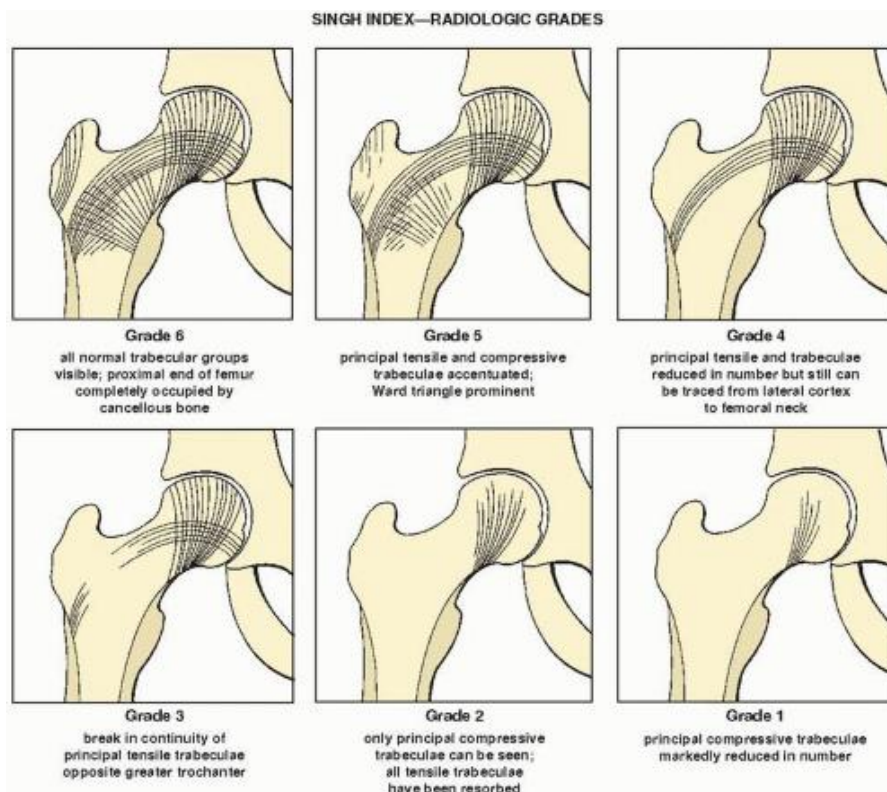


*Figure 15: Singh Index Grades [44].*

The S.I. class assignment is based on the evaluation of the trabecular bone in the proximal femur, through a radiographic analysis, and of the Cortical Index (C.I.), calculated at isthmus's level, expressed as following:

$$C.I. = \frac{a - b}{a} * 100;$$

where  $a$  represents the external femoral diameter and  $b$  the internal medullary cavity (Figure 16). Therefore can be identified three different situations:

- Thin cortical layer corresponds to C.I. smaller than 40;
- Intermediate cortical layer corresponds to C.I. between 40 and 60;
- Thick cortical layer corresponds to C.I. bigger than 60.

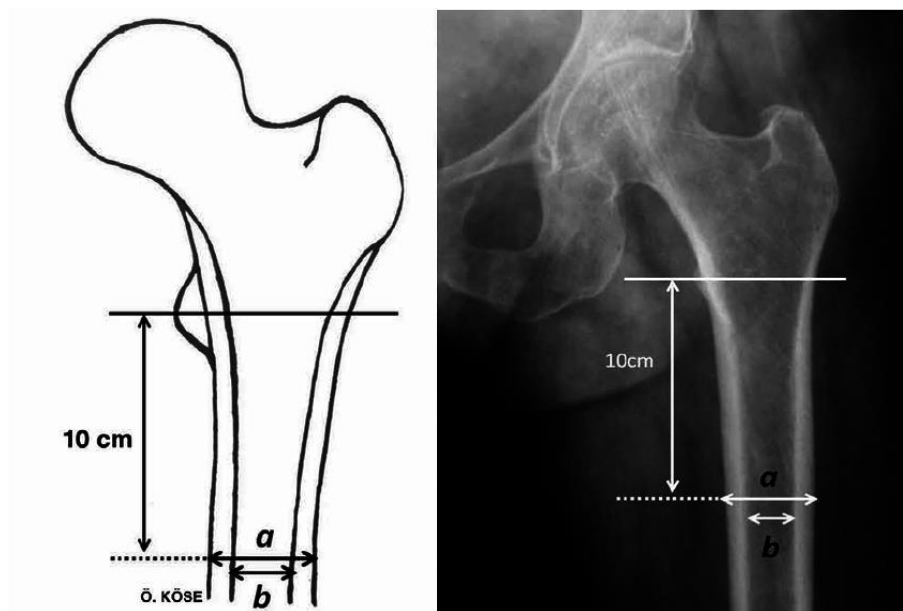


*Figure 16: Representation of the Cortical Index; the point 10 cm above the lesser trochanter is considered as indicator of the beginning of the istmo's area.*

The second main index, used to evaluate the quality and the condition of the bone tissue in analysis, is the Flare Index (F.I) expressed as the ratio between the femoral canal 2 cm above and 10cm below (at the istmo's level) the lesser trochanter; those two components are obtained using an anterior-posterior radiography (Figure 17) [32].



*Figure 17:Representation of the dimensions of interest to calculate the F.I.*

As a result, three different configurations can be observed (Figure 18):

- Champagne-flute with F.I bigger than 4.7;
- Normal with F.I between 3 and 4.7;
- Stovepipe with F.I smaller than 3.

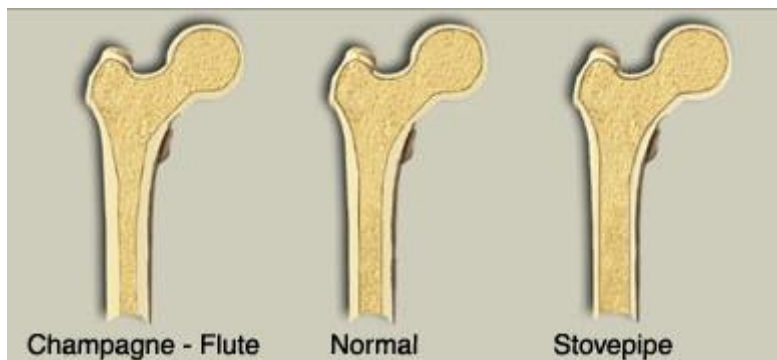


*Figure 18: Representation of the three F.I. configuration [45].*

This index is strictly related to the patient's age. Indeed, it is observed that in patients older than 60 years old the femur assumes a shape close to the stovepipe; this is a consequence of the cortical bone layer thickness reduction [31].



### 2.3.2 Stem Design

Stems [12] can differ one from the other depending on their length, shape and cross section dimension and geometry.

It is possible to identify two main shapes:

- Curved stems (Figure 19), which are bent in order to follow the curve between the femoral neck and shaft since they are inserted through the first one;

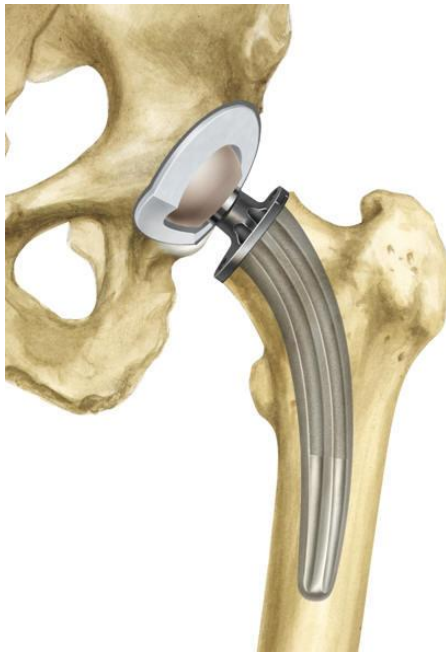


*Figure 19: Curved stem [46].*

- Straight stems (Figure 20), are designed to be inserted from the piriform fossa and have a more anatomical shape into the medullary canal.



*Figure 20: Straight stem.*

Between those two, the straight one are more used and preferred since they guarantee a major stability of the implant, a smoother stress distribution and a minor bending moment at the mid-stem area than the curved ones [33].

Regarding the cross section shape [13], geometry with corners are preferred when in presence of cementless implant since they have been shown to be successful in reducing torsion and to guarantee a major stability. On the contrary circular or elliptical sections are mostly used for cement implants, since in that way the bone removal quantity required is reduced.

Thanks to the introduction of short stems (Figure 21) it has been possible to reduce even more the quantity of bone removed. They are mostly used for primary THA, in order to preserve as much as possible bone tissue in prevision of possible revision.



*Figure 21: Representation of long stem (on the left) and short one (on the right) [12].*

### **2.3.3 Modularity**

Modular implants [7] are multicomponent devices (Figure 22), which have been introduced in the late 60's. Those were designed to allow the surgeon to assemble the prosthesis most suitable for the anatomical situation of different patients by using interchangeable heads and stems of various sizes. Moreover, in case of failures or revisions, by using this kind of implants replacing the individual damaged parts and not the whole implant is possible.



*Figure 22: Modular Hip Prosthesis [12].*

Modular designs have some direct functionality advantages [13] over monobloc ones since they allow adjustment of the cervico-diaphyseal angle, lateral offset, neck anteversion/length and lower limb length independent of stem dimension and geometry. Moreover they introduce a major versatility, ease replacement during revisions, as previously said, and possibility of using different materials for the components.

But there are also some disadvantages:

- By increasing the number of components, the number of surfaces which interacts increase too. This has a direct effect on the number of debris released in the surrounding environment and third body wear.
- If different materials are used, it is important to evaluate the fretting at the interfaces [34];
- During the assembling of the different parts residual stresses could be generated.

## **2.4 Introduction to the Finite Element Analysis**

The finite element analysis [36] is accomplished by using suitable software; in this study the one used is Abaqus, a software which is able to perform static, dynamic, fluid dynamics and electromagnetic analysis.

Each complete finite element analysis consists of 3 separate steps (Figure 23):

- *Pre-processing* or *Modeling*: the element is chosen and the material properties are defined; it is followed by the discretization of the domain (*Meshing*) and assignment of the initial and/or boundary condition;
- *Solution*: acquirement of the solution;
- *Post-processing*: visualization and analysis of the results.

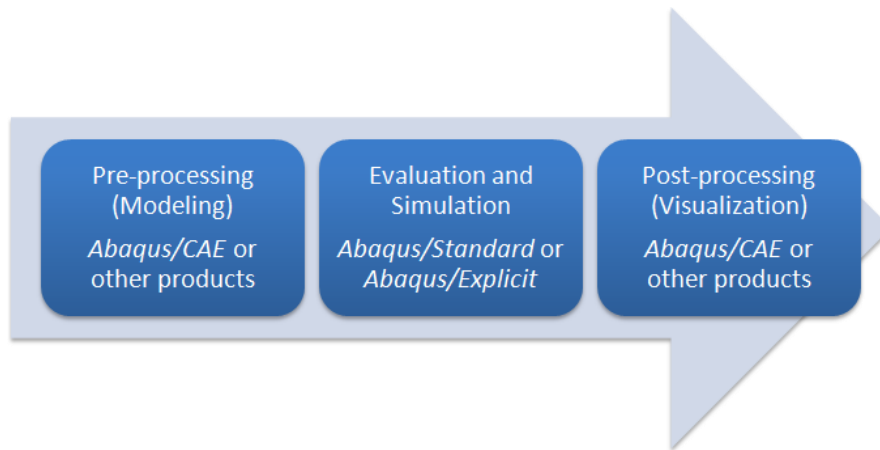


Figure 23: Flowchart of the steps necessary to complete a finite element analysis [37].

The pre-processing phase is the stage that requires most time; the object, which has to be analyzed, can be mono, bi or tridimensional and it can be either realized directly in Abaqus or imported as a CAD. After defining the geometry property, the material one are assigned; those define the mechanical behaviour of the material, which can be elastic/anelastic, isotropic/anisotropic, time and/or temperature dependent/independent. It is then necessary to define the loads acting on the structure and the boundary conditions.

Regarding the process of parametrization of a finite element model of a femur, a few study exists in literature concerning this topic. K. F. Klein et al. [38] realized a default model by using statistical model that predicts the femur geometry, parameterizing it respect the femur length, BMI and associated age; the study demonstrated that the most relevant variation in terms of results were obtained by modifying the BMI, concluding that modifications of the other parameters have not a relevant effect on the results. In another study, D. P. Nicoletta et al. [39] implemented a statistical shape modeling based method to develop a parametric finite element representation of the proximal

femur shape and bone density distribution of a group of cadaveric femurs. The last work highlighted in this paper is the one fulfilled by M. Armand et al. [40]; in this work the parametrization was achieved only on the diameter of the cortical and spongy part, where the second one is connected to the first one with an algorithm which consider also bone density.

### **3 AIM OF THE STUDY**

Nowadays different FE models of the femur have been introduced in order to study the effect of different loads and material properties in hip arthroplasty.

However none of these allow the user to modify the model's geometry, starting from a default model.

In order to do that a parametric model has been realized in Abaqus (SIMULIA, Johnston, RI, USA), by using purposely developed Python scripts. By using them, the user, by inserting a series of parameters which differ for each section below, is now able to modify the:

- Geometry;
- Material properties;
- Acting loads;
- Mesh.

Another option that has been given to the user is the possibility to simulate the implantation of a hip prosthesis in the model. Regarding this aspect, a gold standard model has been realized, which consider a better interaction between the surfaces of the prosthesis and the bone, a feature which has not been possible to apply to the parametric model.

The results have been then compared, in order to analyze the difference between the two models.

Same process has been used with an analytical model with the purpose of validate the study and the results achieved; those have been obtained in term of stresses acting on the femur by modifying three main parameters:

- Loads, which differs according to the current movement simulation that is being analyzed (stance, walking, running, falling, ecc.);

- Material properties, depending on the kind of bone is being analyzed (healthy or osteoporotic);
- Femoral geometry.

## **4 MATERIALS & METHODS**

### **4.1 FE Model Development**

In order to realize the parametric model, as a first step it has been necessary to realize a default model; this one has been built by using a series of points obtained in a previous study, which define the geometry of the cortical and spongious part.

New femoral geometries are then realized by modifying the default femur using appropriate parameters, which are calculated on the radiographic image of a specific patient. Those are requested to the user by an easily usable interface, which, moreover, allows to him to manage the material, loads and the element size of the mesh. In addition the user has also the possibility to apply or not a prosthesis to the model.

The realization of the FE model is described in details in the following chapters.

#### **4.1.1 Points Acquisition**

The acquisition of the points, that are used to realize the model in Abaqus, has been obtained in a previous study by using the software described as follows.

The first computer program is necessary to obtain 2-dimensional slices the body part of interest and analyze the properties of the materials. This role is fulfilled by the CT (Computed Tomography) scanner [11]; with this machine it is possible to get X-ray images from different angles of specific areas. The different tissue composition is acquired by analyzing the ray transmission through the patient, caused by a different absorption level. For this purpose, on the opposite side from the X-ray

source, detector is placed, which collects the coming out radiations from the patients and sends them to a computer (Figure 24).

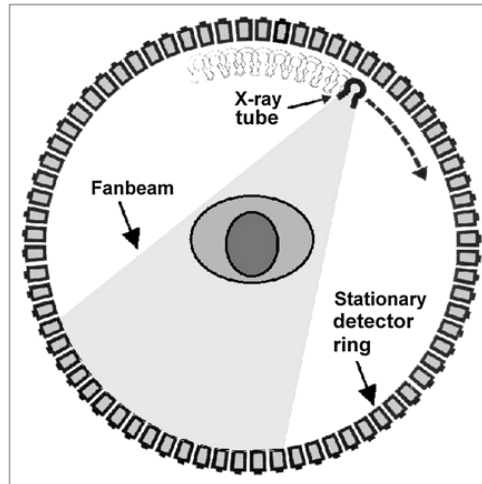


*Figure 24: Illustrating scheme of the operating principle of the CT scanner.*

The computer calculates the attenuation of the X-ray for all voxels, i.e. the 3-dimensional volumetric elements in which the tissue has been divided. These calculated attenuation values are then represented as gray levels in a 2-dimensional image of the slice, usually called pixel.

The main advantage of this method is that it allows to achieve informations either about the geometry and structure property.

The second piece of software is necessary to regroup all the information achieved and to rebuild the 3-dimensional shape of the body part of interest, in this case the femur, by assembling one after another the virtual slices of the CT scan, connecting them in the same order as they have been obtained. One of the most common and used is MIMICS (Materialise's Interactive Medical Image Control System), produced by the company MATERIALISE NV Software, as well also SIMPLOWARE ScanIP, developed by the company Synopsys.

To be more precise, in this study [15] the CT scans have been applied to a sawbone and the 3D model has been obtained with MIMICS.

The 3D model realized has then been imported in Solidworks CAD 3D (Dassault Systèmes SolidWorks Corp.) where the femur has been divided in four main regions (Figure 25):



- Femoral stem (A);
- Throcanteric Region (B);
- Femoral Neck (C);
- Femoral Head (D).

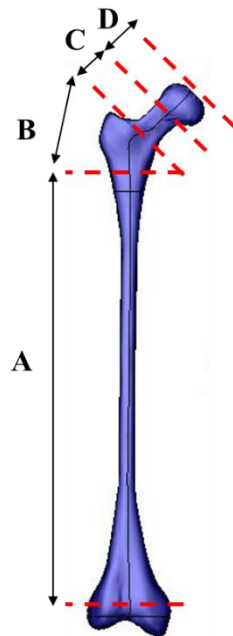


Figure 25: 3D model in Solidworks and representation of the four region of interest.

After that, for each region a certain number of transversal planes have been created, in particular:

- 40 parallel ones for the femoral stem;
- 14 for the throcanteric region, with different inclinations with respect to a common point (*Ref "4.12 Geometry Realization"*). To be more precise, each plane is inclined of  $3.1^\circ$  respect the previous one, so that the inclination of the last plane is  $43.4^\circ$ ;
- 10 for the neck region. All the planes result parallel to the last one of the throcanteric region;
- 10 for the femoral head region in the cortical part and 9 in the spongious one. As well as for the neck region, all the planes are parallel to the last one of the throcanteric region.

For each one of these planes, 18 equispaced points have been identified on the external surface; their coordinates, expressed in cilindrical coordinates, have then been saved in “.txt” file.

### 4.1.2 Geometry Realization

The first step before importing the points in Abaqus is to convert their coordinates from cylindrical  $((R, \vartheta, z))$  to rectangular ones  $((x, y, z))$ ; the following equation are applied:

$$\begin{cases} x = R \cos \vartheta \\ y = R \sin \vartheta \\ z = z \end{cases}$$

While the points of the femoral stem region are already referred to a global coordinate system, the ones of the other regions are referred to a local one; it is then necessary to convert them to the global system. Considering the following geometry (Figure 26):

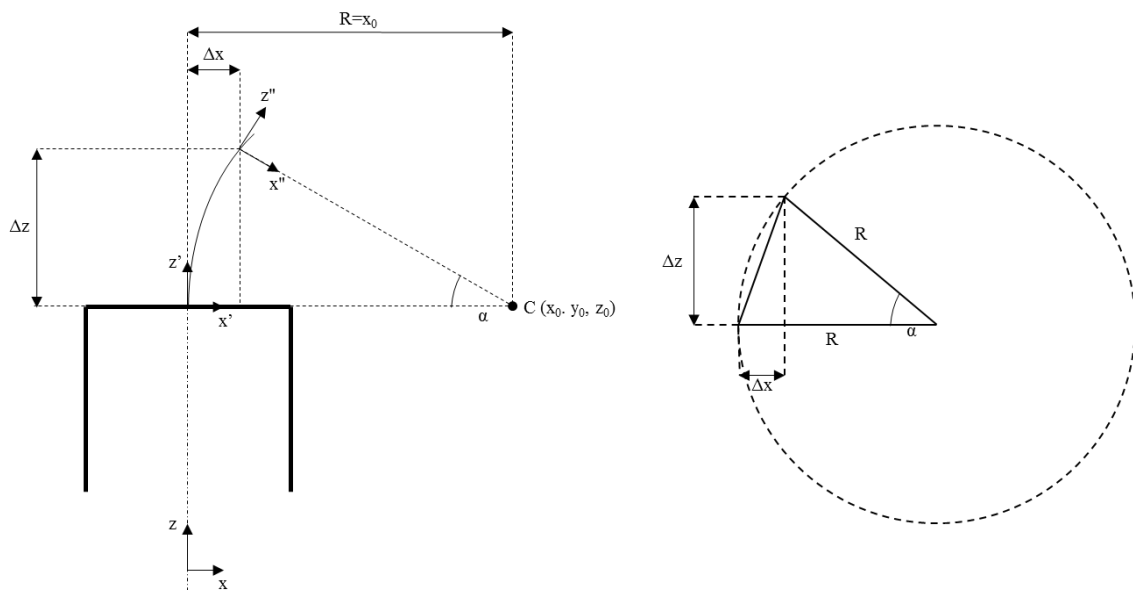


*Figure 26: C represents the fixed point used to build the planes of the trochanteric, neck and head area; R coincide with  $x_0$ , since the center of the circle is in C;  $\Delta x$  and  $\Delta z$  represent respectively the translation of the local coordinate system along the x and z axis of the global one.*

the equations to obtain the coordinates of the points referred to a global system are the following:

$$\begin{cases} x = R(1 - \cos \alpha) + x'' \cos \alpha + z'' \sin \alpha \\ y = y'' \\ z = z_0 + R \sin \alpha - x'' \sin \alpha + z'' \cos \alpha \end{cases}$$

The points were then imported in Abaqus and connected by using the function *Wire*.

By using the comand *ShellLoft* the surfaces between the wires was generated while the function *CoverEdges* was used to create the surface at the bottom and at the upper part of the femur in order to obtain a closed volume. The result on the cortical part is shown in Figure 27:

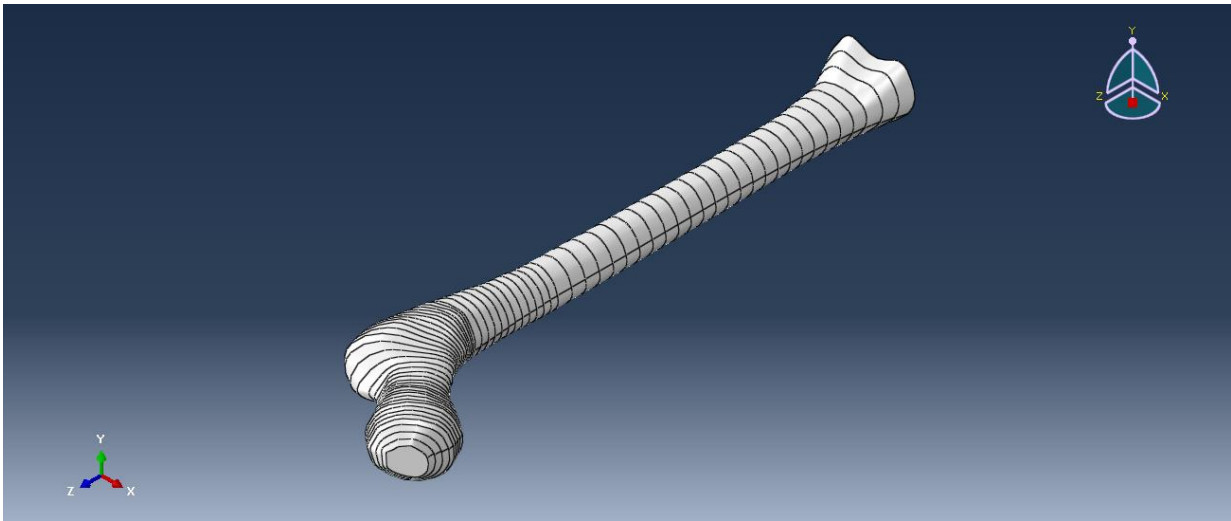


*Figure 27: Representation of the cortical part of the femur.*

In order to assemble the two parts, the spongious and cortical one, the two instances of those were first defined and after that the function *Merge* was (Figure 28).

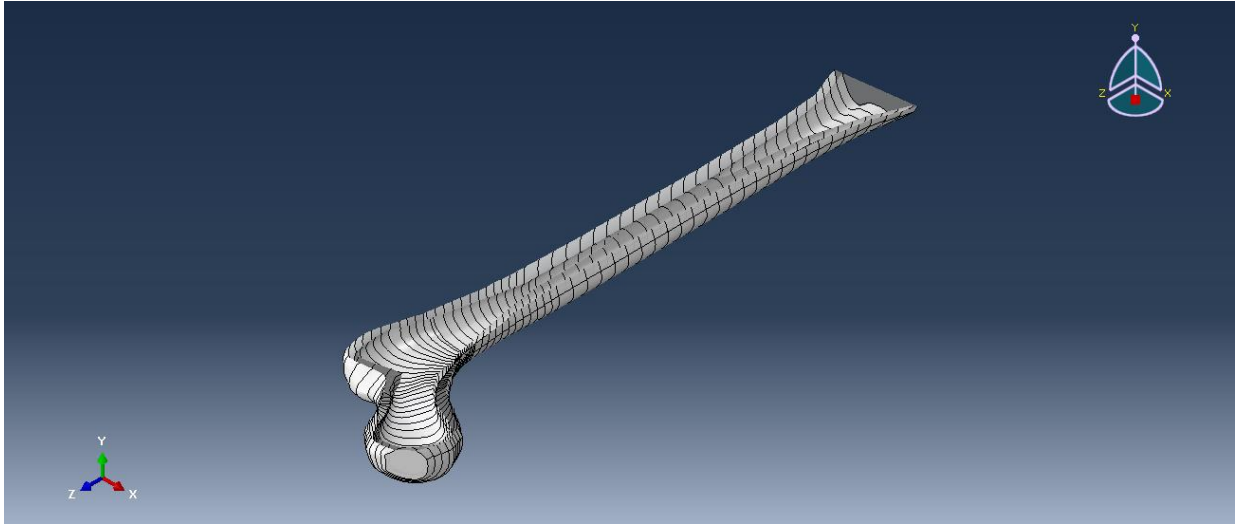


*Figure 28: Representation of a section of the model along the y-axis with the purpose to highlight the presence of the two different parts.*

### **4.1.3 Material Realization**

The bone tissue, considering its material properties, can be distinguished in cortical and cancellous. These two have different localization into the femur (Figure 29).

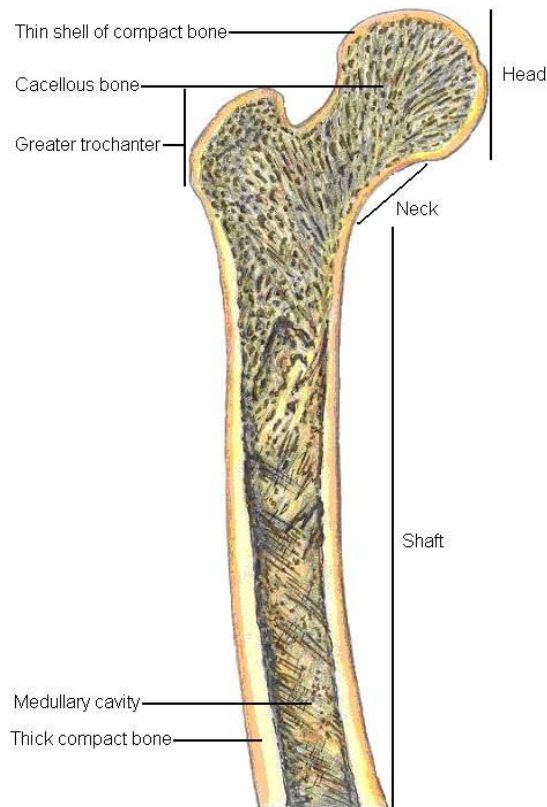


*Figure 29: Location of cortical and cancellous bone in the femur.*

They also have different mechanical properties; those are subjected to modifications in presence of a non healthy bone tissue, as for an osteoporotic one (Table 1) [35]. It should be noted that these parameters refer to a coordinate system where the z-axis (reference number 3) is oriented as the anatomical axis and pointing to the femoral head, the x-axis (reference number 1) lies in the frontal plane while the y-axis (reference number 2) in the sagittal one. Moreover in this model, those axis coincide with the ones of the global coordinate system.

<i>State</i>	<i>Type</i>	<i>Mechanical Properties</i>		
		<b>E<sub>1-2-3</sub></b> <b>[GPa]</b>	<b>v<sub>12-13-23</sub></b>	<b>G<sub>12-13-23</sub></b> <b>[GPa]</b>
<u>Healthy</u>	<u>Cortical</u>	11.5	0.51	3.80
		11.5	0.31	4.39
		17	0.31	4.39
	<u>Cancellous</u>	2.13	0.3	0.82
<u>Osteoporotic</u>	<u>Cortical</u>	7.82	0.51	2.59
		7.82	0.31	2.98
		11.56	0.31	2.98
	<u>Cancellous</u>	0.724	0.3	0.28
<u>Osteopenic</u>	<u>Cortical</u>	9.66	0.51	3.19
		9.66	0.31	3.68
		14.280	0.31	3.68
	<u>Cancellous</u>	1.427	0.3	0.55

Table 1: Bone tissue materials properties for a healthy, an osteoporotic and an osteopenic patients.

Where G, the shear modulus, is calculated as follows:

$$G_{i,j} = \frac{E_i}{2 * (1 + \nu_{i,j})};$$

In order to assign the material properties to a specific part, as a first step the cortical and spongius properties were defined under the *Material* section. In the default case the first one is orthotropic while the second isotropic (Table 1). After that, under the *Section* option, the two section typologies

have been defined, one for the cortical and one for the spongy part; in both the two cases those are homogeneous and solid.

The properties were assigned to the parts by using the voice *Section Assignments* and a coordinate reference system was assigned by using *Assign Material Orientation*, under the voice *Property*.

These steps are summed up in the following block diagram (Figure 30).

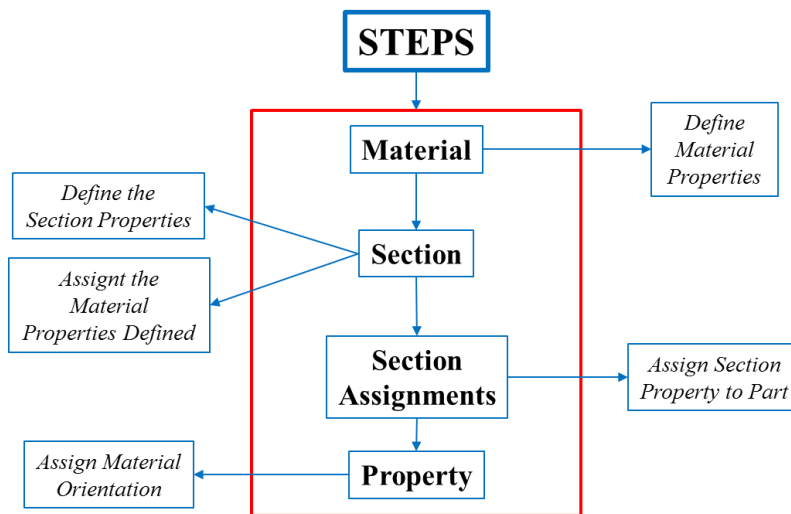


Figure 30: Flowchart of the steps necessary to assign the material properties.

The result of the assignment is shown in Figure 31, where the green area represents the cortical part while the white area the spongy one.

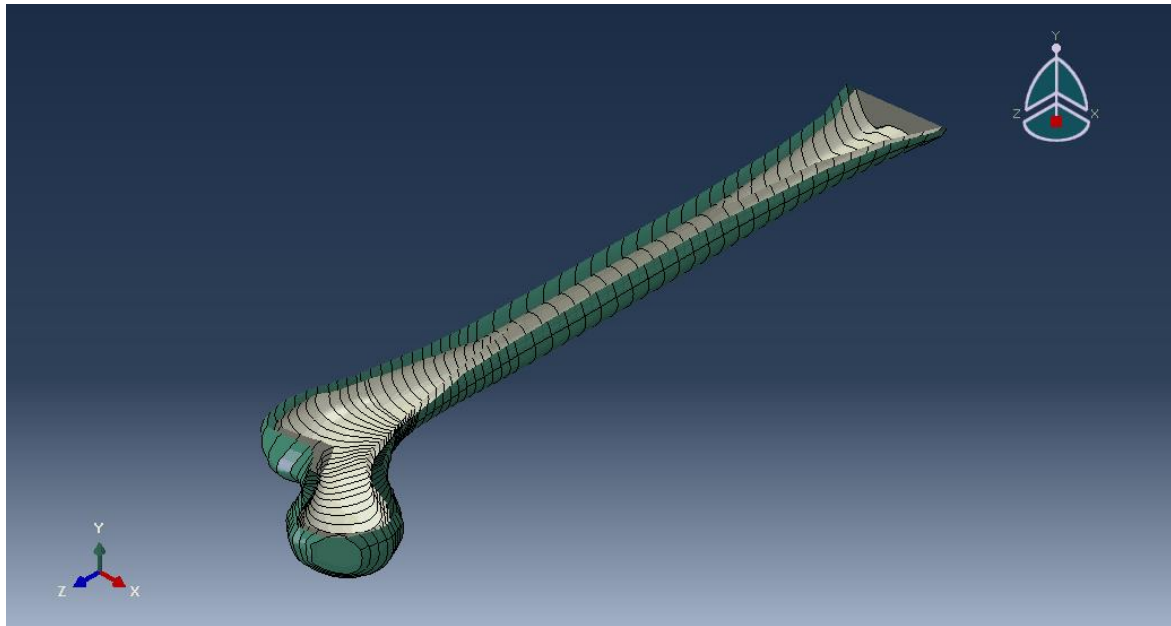


Figure 31: Representation of the cortical and spongy part.

#### 4.1.4 Load and Costraints Assignment

In order to simulate various movements, different loads[14] were applied on the femoral head (Table 2):

<b>MOVEMENT TYPE</b>	<b>R<sub>x</sub> [N]</b>	<b>R<sub>y</sub> [N]</b>	<b>R<sub>z</sub> [N]</b>
<b>Walking</b>	535.72	-342.48	-1747.18
<b>Stance</b>	575.78	-120.8	-1947.12
<b>Cycling</b>	242.04	-202.49	-651.75
<b>Stand Up</b>	649.82	-203.74	-1428.38
<b>Stairs Down</b>	774.11	-771.02	-2852.39
<b>Stairs Up</b>	712.3	-565.73	-1999.57
<b>Sit Down</b>	460.18	-245.02	-1246.76
<b>Jogging</b>	777.18	-752.73	-2845.19

Table 2: Hip loads acting on the left femur; those reported are the maximum values measured in each activity.



The data are based on in vivo measurements in ten active subjects during nine frequent activities of daily living. Those reported in the table represent the average of all the values measured on the ten patients, after normalizing the body weight to 75 kg, and are referred to a left leg.

The following muscle forces [15] have been also introduced, for the purpose of obtaining a reliable model as close as possible to emulate a physiological response of the limb (Table 3).

<b>MUSCLE TYPE</b>	<b>R<sub>x</sub> [N]</b>	<b>R<sub>y</sub> [N]</b>	<b>R<sub>z</sub> [N]</b>
<b>Gluteus Maximus</b>	236.8	36.8	334.4
<b>Gluteus Medius</b>	234	105.3	207
<b>Gluteus Minimus</b>	102	35	136
<b>Ilio-Psoas</b>	0	-160.2	158.4
<b>Piriformis</b>	113.5	62.4	38.4
<b>Adductor Magnus</b>	76.36	24.84	170.2
<b>Adductor Minimus</b>	56.4	-11.7	36.9
<b>Vastus Lateralis</b>	0	153	-708.7

*Table 3: Muscle static forces.*

On the contrary, those muscles have been excluded, since their insertion point is at the level of the knee, which is not included in the model realized:

- Femoral Biceps;
- Gracilis;
- Gastrocnemius Lateral;
- Gastrocnemius Medial.

The loads, realized under the voice *Load* in Abaqus, were not directly applied to the surface; instead a number of reference points equal to the number of loads of interest was realized.

The forces were then applied to these point and those have been connected to the surface of interest by using the *Constraints* function. It is actually possible to choose between different kinds of constraints;

the one used in this case has been the *Coupling*, with a *Structural Distributing* option, which guarantees a uniform distribution of the load on all the surface selected.

Regarding the surfaces to which the points have been connected, those were properly realized with the function *Partition Face: Sketch*, which creates a partition. This procedure was accomplished in order to reproduce in a more accurate way the insertion areas of the muscles or, in the case of the hip, the contact area between the acetabulum and the femoral head.

A similar process was used to realize the boundary condition; this one was an encastre applied at the bottom of the femur. It emulated the experimental condition used to test in laboratory the femur where the encastre [7] is achieved by using a cup containing cement in which the condyles part is inserted (Figure 32).

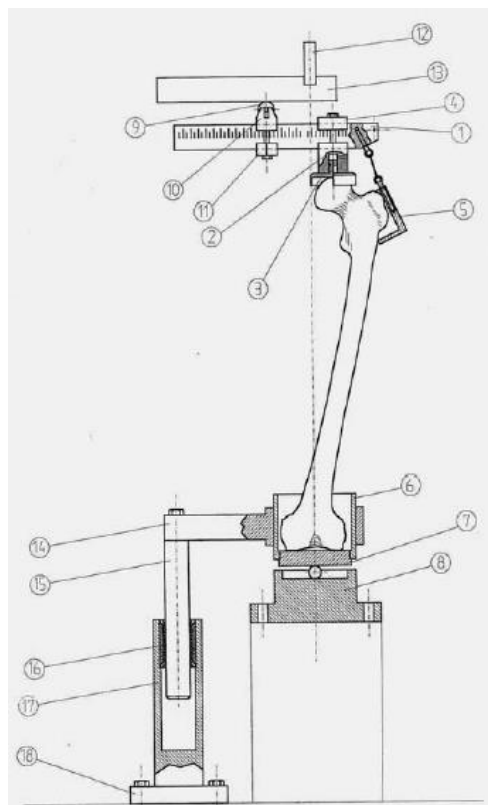


*Figure 32: Experimental set up to test femur properties.*

As a first step, the encastre was defined under the option *BCs* and it was then applied to one of the reference point; this one has been connected to the surface of interest but the option *Kinematic*

*Distribution* was used this time, which has to be used specifically in this case since it doesn't allow any relative motion among the constrained degrees of freedom.

The result of all this procedure is shown in Figure 33:

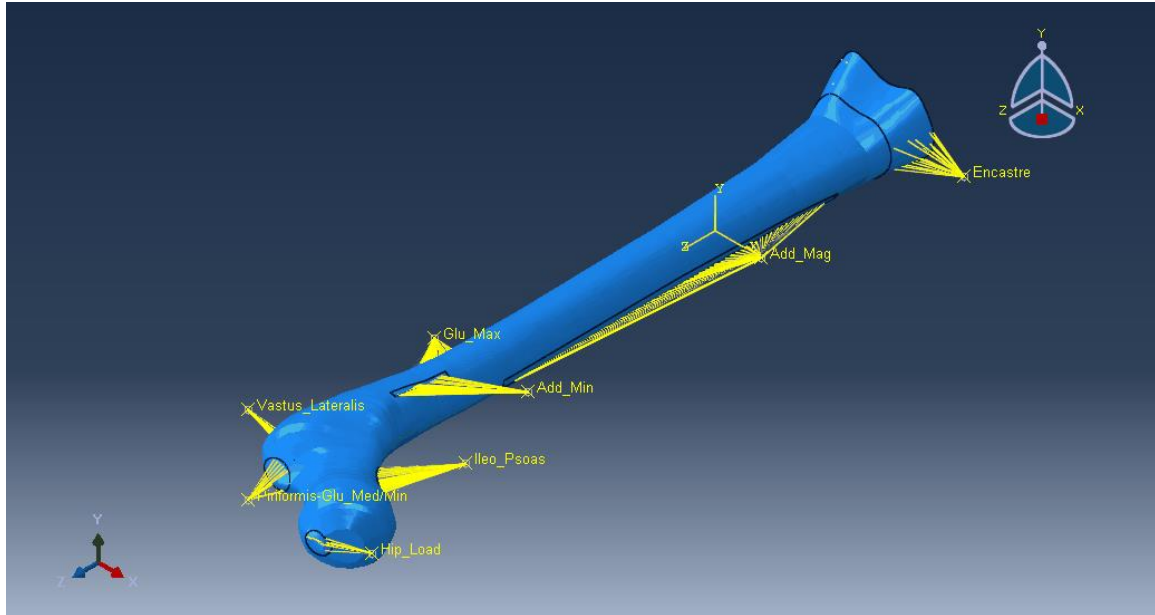


*Figure 33: Representation of the forces acting on the structure and their insertion areas.*

The areas of the muscles on the femur were realized considering their anatomical insertion (Figure 34) and where then realized manually in Abaqus:

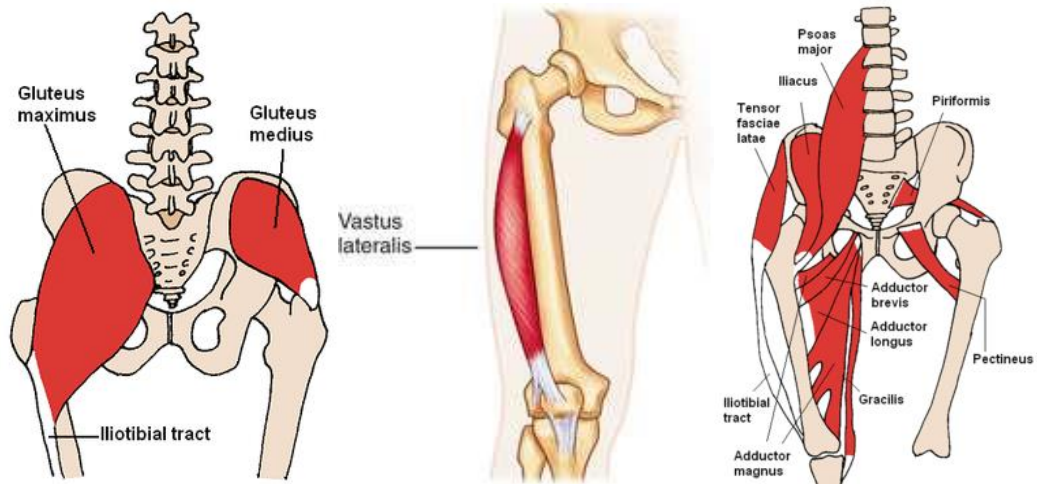


Figure 34: Muscles anatomic insertion areas.

#### 4.1.5 Mesh

The element chosen to mesh the model is a solid linear tetrahedral one (Figure 35).

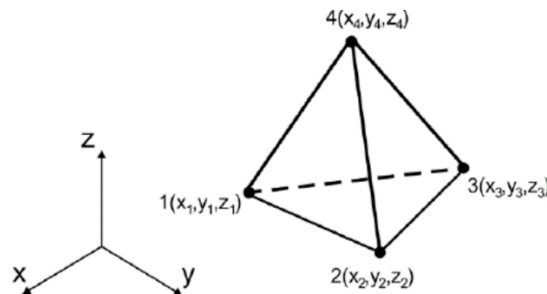
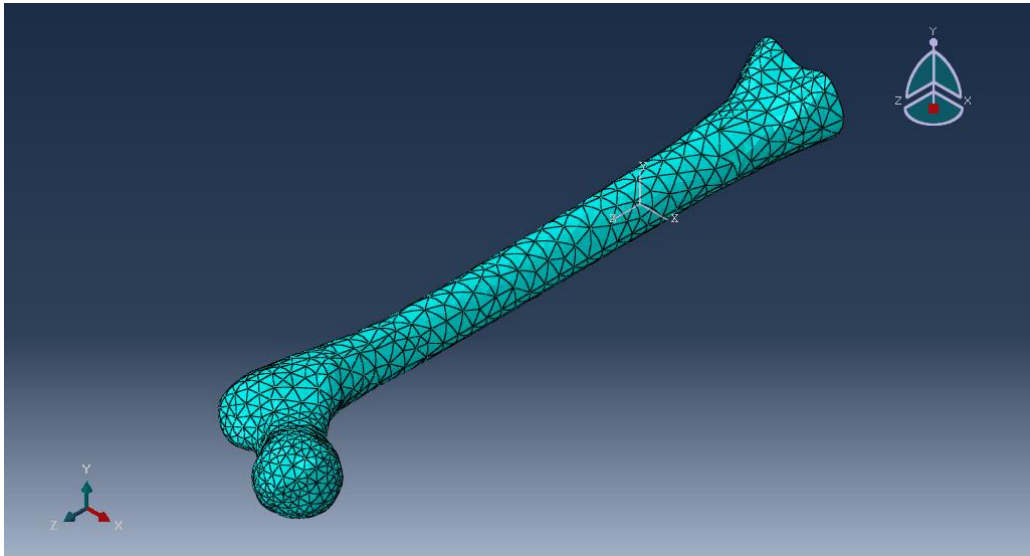


Figure 35: Representation of a linear tetrahedral element.

Under the *Mesh* section the following options were selected in order to obtain the mesh:

- *Assign Element Type*: a standard *Element Library* and a linear *Geometric Order* were chosen;
- *Assign Mesh Controls*: a tetrahedral element type was assigned to all the model;
- *Seed Edges*: the element size has been defined, in particular 5 is the *Approximate Element Size* in the default model;
- *Mesh Part Instance*.

The result at the end of the meshing process is shown in Figure 36.



*Figure 36: Mesh representation.*

## 4.2 Parametric Model

### 4.2.1 Modification of Geometry

In order to modify the geometry of the default femur to obtain the patient-specific one, the following parameters (Figure 37), which are the most clinically relevant and easily measurable, have to be selected by the user:

- $L_F$  is the femoral length. It has to be taken considering as extremities the insertion point of the proximal articular cartilage of the distal femoral articulation and the point between the ending of the small and the beginning of the great trochanter;
- $R_H$  and  $\Phi_H$  are the femoral head radius and diameter, respectively;
- $I_\Phi$  is the femoral diameter. It has to be taken at the level of the isthmus;

- $I_{\text{Thickness}}$  is the femoral thickness. It has to be taken at the level of the isthmus;
- $\alpha$  is the neck slope;
- $\gamma$  represents the angle between the anatomical and the mechanical axes, considering as starting point of the latter one the insertion point of the proximal articular cartilage of the distal femoral articulation.

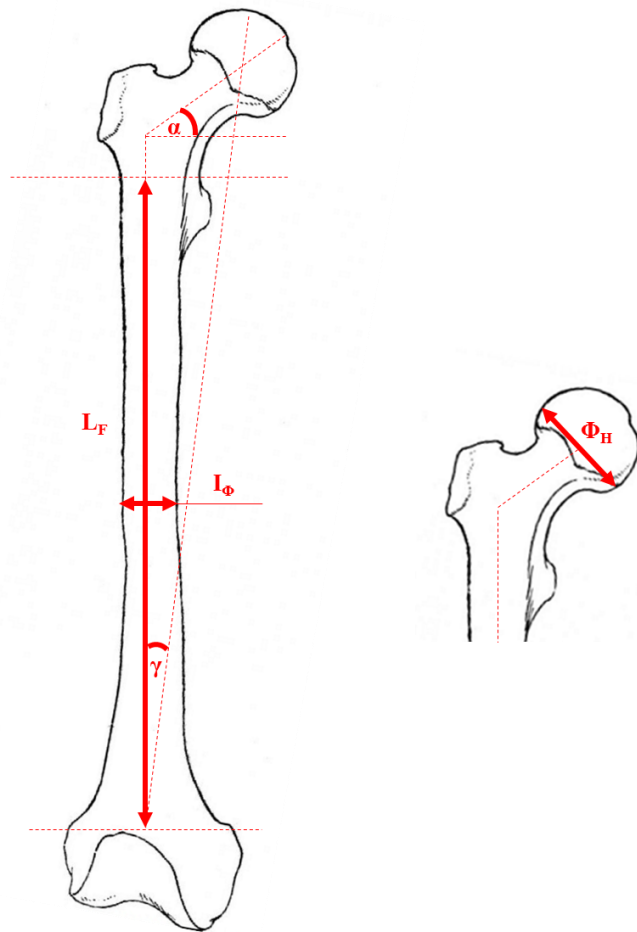


*Figure 37: Representation of the parameters of interest.*

Another parameter was calculated indirectly, which is the  $L_N$  (Neck Length), shown in Figure 38.

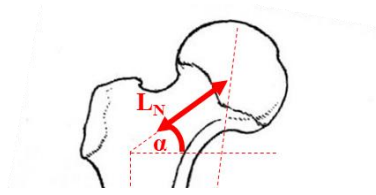


Figure 38: Representation of the neck length.

In order to do that, an analytical model of the femur was realized (Figure 39).

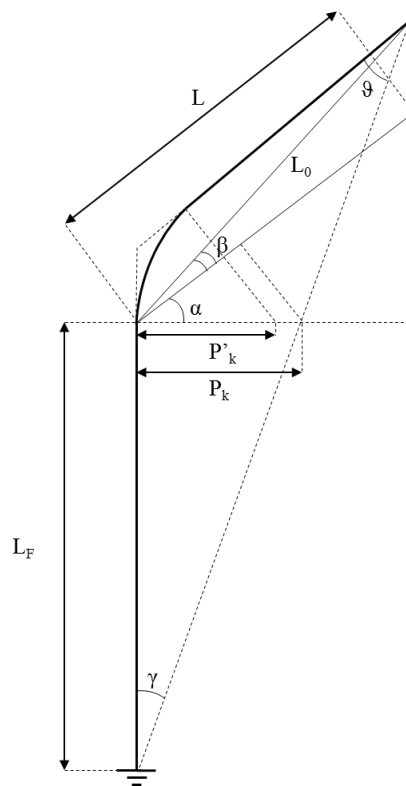


Figure 39: Analytical model with the purpose of representing the femur.

The following hypothesis was assumed as legitimate (Ref. "5.1 Validation of the Model"):

$$\cos \beta \cong 1;$$

The consequence of this assumption is that  $L \cong L_0$ , since  $\beta \rightarrow 0$ . The outcome in the model was that the real profile of the trochanteric-neck part can be considered coincident with the straight line which components are  $k_1$  and  $k_2$  (Figure 40):

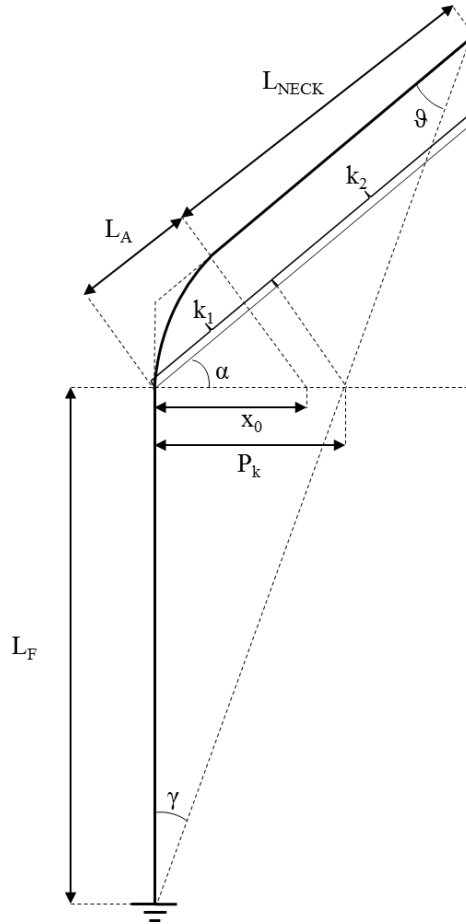


Figure 40: Analytical model to calculate  $L_{Neck}$  after considering valid the hypothesis.

By using appropriate trigonometric considerations, the neck's length ( $L_{NECK}$ ) was obtained as follows:

$$L_{Neck} = k_2 + (k_1 - L_A);$$

where  $x_0$ , which appears in the model (Figure 40), is a fixed value, corresponding to 45.87 mm respect the global coordinate system; the other variables have been calculated by using these equations:



$$\begin{cases} k_2 = \frac{L_F * \tan \gamma * \sin \alpha}{\tan \vartheta} \\ k_1 = L_F * \tan \gamma * \cos \alpha \\ L_A = x_0 * \cos \alpha \end{cases}$$

The parameters inserted by the user are compared to the ones of the default model; a coefficient is then calculated and it is used to modify the coordinates of the points of interest before representing them into the Abaqus 3D space.

All these coefficients are discussed one by one below:

- $Coef f_{Stem_{Length}} = \frac{L_F^{User\ Defined}}{L_F^{Default\ Model}}$

It is induced due to a variation of the femoral length ( $L_F$ ). It affects all the z-coordinates of all the region of the model. To be more precise, the z-coordinates of the femoral stem part have to be multiplied for the coefficient, while the ones of the other region have to be translated:

$$StemPart : z[i] = z[i] * Coef f_{Stem_{Length}}$$

$$OtherAreas : z[i] = z[i] + \Delta_z$$

where  $\Delta_z$  represents the difference between the value of the z coordinates of the last plane of the stem after and before the application of the coefficient;

- $Coef f_{Stem_{Diameter}} = \frac{I_\Phi^{User\ Defined}}{I_\Phi^{Default\ Model}}$

A variation of the femoral stem diameter at the level of the isthmus ( $I_\Phi$ ) has as a consequence a variation of all the x and y-coordinates of the model, in order to preserve a correct shape of the femur. The following equation has been properly implemented:

$$\begin{cases} x[i] = x[i] * Coef f_{Stem_{Diameter}} \\ y[i] = y[i] * Coef f_{Stem_{Diameter}} \end{cases}$$

Actually this equation has to be applied twice, since two coefficients have to be calculated in this way, one for the spongy and one for the cortical part.

It is also important to specify that the  $I_{\Phi}^{\text{Default Model}}$  has been calculated as the mean value of the diameters measured on 5 different adjacent planes at the isthmus level. Moreover the diameter of each plane is as well the mean value of the diameters calculated on that single plane;

- A variation of the femoral neck slope ( $\alpha$ ) affects all the areas except for the femoral stem one. In this case a coefficient is not calculated and to obtain the modification induced, the equation expressed to convert a point from a local coordinate system to a global one (*Ref. "4.2.1 Geometry Realization"*) are used directly in Python, since the points of those areas have been imported before being converted.

- By modifying the angle between the anatomical and mechanical axis ( $\gamma$ ) the effect induced is a modification of the femoral neck length ( $L_{\text{Neck}}$ ). A coefficient which represents the ratio between the  $L_{\text{Neck}}^{\text{Used defined}}$  and the  $L_{\text{Neck}}^{\text{Default Model}}$  is then calculated. This procedure is similar to the one applied in presence of variation of the femoral length; the only difference is that in this case the coordinates are the ones referred to a local coordinate system, which are then converted by using the parameter  $\alpha$ .

Again, the z''-coordinates of the neck area are multiplied by the coefficient of interest while the ones of the femoral head are just translated. The coordinates of all the other areas are not affected by this parameter.

- $Coef f_{HeadRadius} = \frac{R_H^{User Defined}}{R_H^{Default Model}}$

It affects only the femoral head region; the following equation is used:

$$\begin{cases} x[i] = (x[i] - x_0) * Coef f_{HeadRadius} + x_0 \\ y[i] = (y[i] - y_0) * Coef f_{HeadRadius} + y_0 \\ z[i] = (z[i] - z_0) * Coef f_{HeadRadius} + z_0 \end{cases}$$

where  $x_0$ ,  $y_0$  and  $z_0$  represents the coordinates of the center of the local coordinate system, placed at the center of the last plane of the neck area.

#### 4.2.2 User Interface

The user interface realized is run directly on Abaqus CAE by running a properly launch file in the *Kernel Command Line Interface* and allows the user to manage the model's:

- geometry;
- material properties;
- hip load;
- mesh.

The logical scheme of the interface is represented in the following flow diagram (Figure 41).

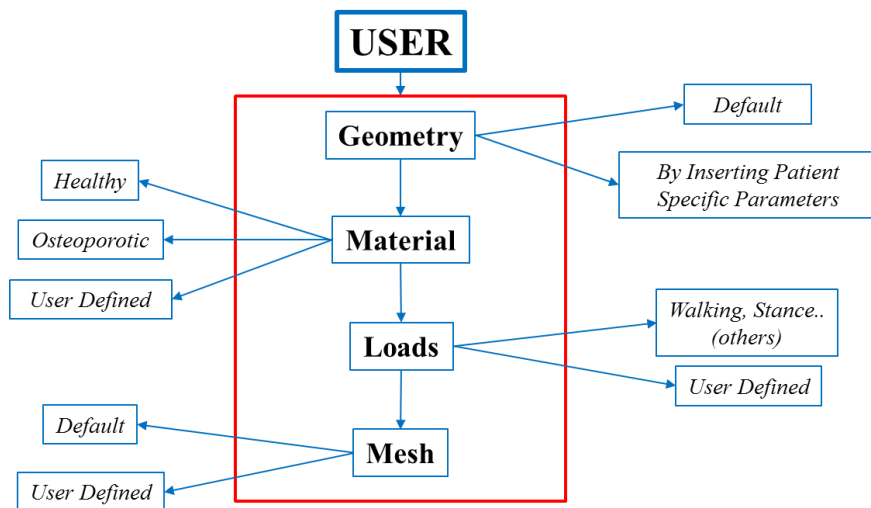


Figure 41: Flowchart to represent the logical scheme of the interface.

For each one of these, the user can choose between:

- using default's settings;
- defining specific parameters.

The parameters requested are different for each section:

- *Geometry*: as previously explained (Ref. “4.2.1 Geometry Realization”) in order to modify the geometry of the default model to obtain the one of interest, 6 parameters are requested (Figure 42) which are the femoral stem length ( $L_F$ ), femoral thickness ( $I_{Thickness}$ ) and diameter ( $I_\Phi$ ) at the isthmus level, femoral head radius ( $R_H$ ), the neck slope ( $\alpha$ ) and the angle between the anatomical and mechanical axis ( $\gamma$ );

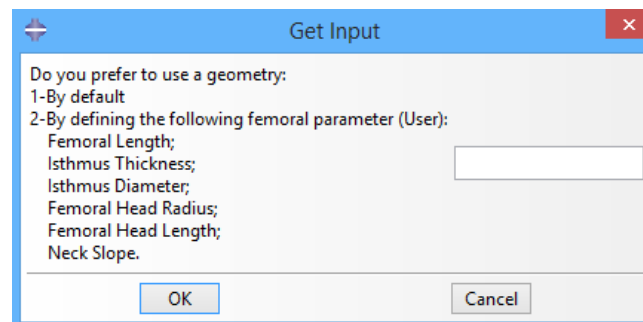


Figure 42: Geometry interface.

- *Material*: the user interface first proposes to choose between the properties of physiologic bone, osteoporotic bone or to provide user-defined properties (Figure 43). If the latter option is chosen, it is first necessary to define the property of the material, either for the spongy and the cortical part; it is then possible to choose between isotropic or transversal orthotropic. Depending on the answer of the user, it is then requested to type the Young Modulus ( $E$ ) and the Poisson Coefficient ( $\nu$ ), if isotropic properties have been chosen, or the Young Modulus ( $E$ ) in the three directions, as well for the Poisson Coefficient ( $\nu$ ) and the Shear Modulus ( $G$ ), if transversal orthotropic properties have been chosen;

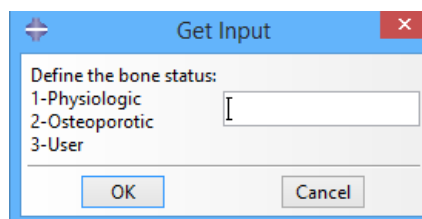


Figure 43: Material interface.

- *Loads*: again, either a pre-defined load case or user-defined loads can be selected, acting in any case on the femoral head (the muscle forces are not manageable). By choosing the user defined option, the parameters requested for this section are the three direction of the force of interest respect the global coordinate system (Figure 44);

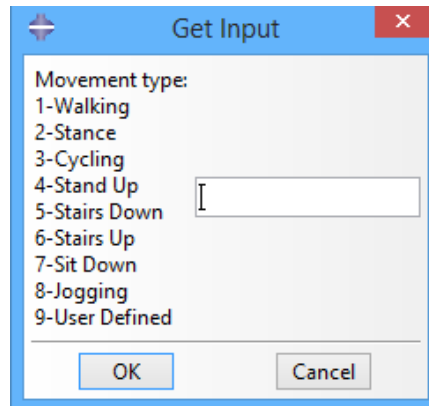


Figure 44: Load interface.

- *Mesh*: for this part the only parameter requested is the (average?) element size that is going to be used to mesh the model (Figure 45).

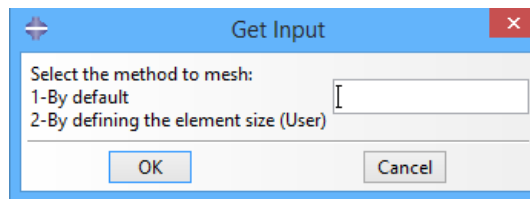


Figure 45: Mesh Interface.

### 4.2.3 Prosthesis (THA) Addition – Femoral Head Excluded

The user has actually another possibility with respect the ones previously described; indeed, the interface realized allows, if required, implanting a hip prosthesis into the femur. In this case too, it is possible to opt for a default option or to define the mechanical properties of the above-mentioned. The flow diagram shown in the previous chapter can be then updated as follows (Figure 46):

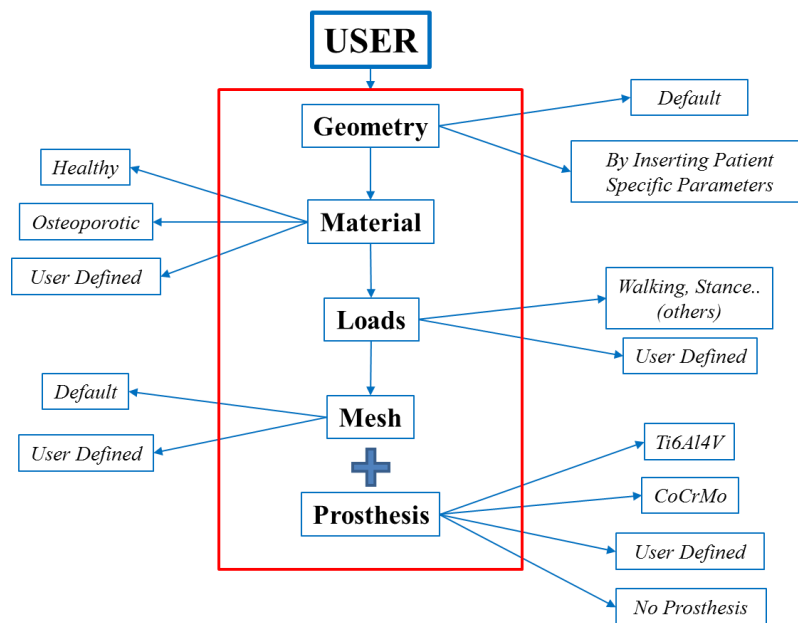
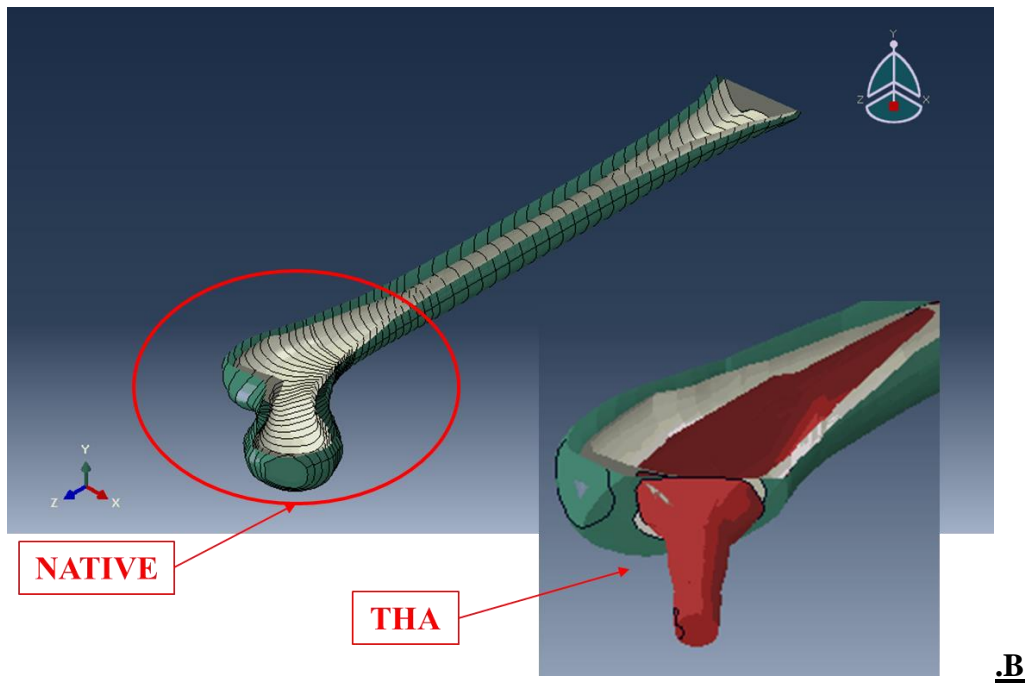
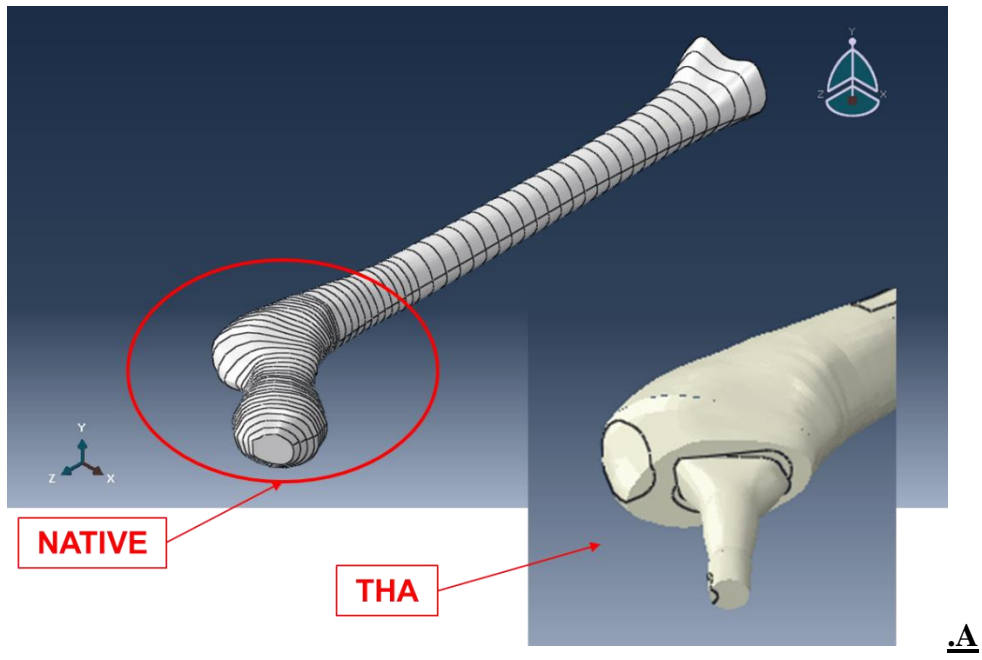
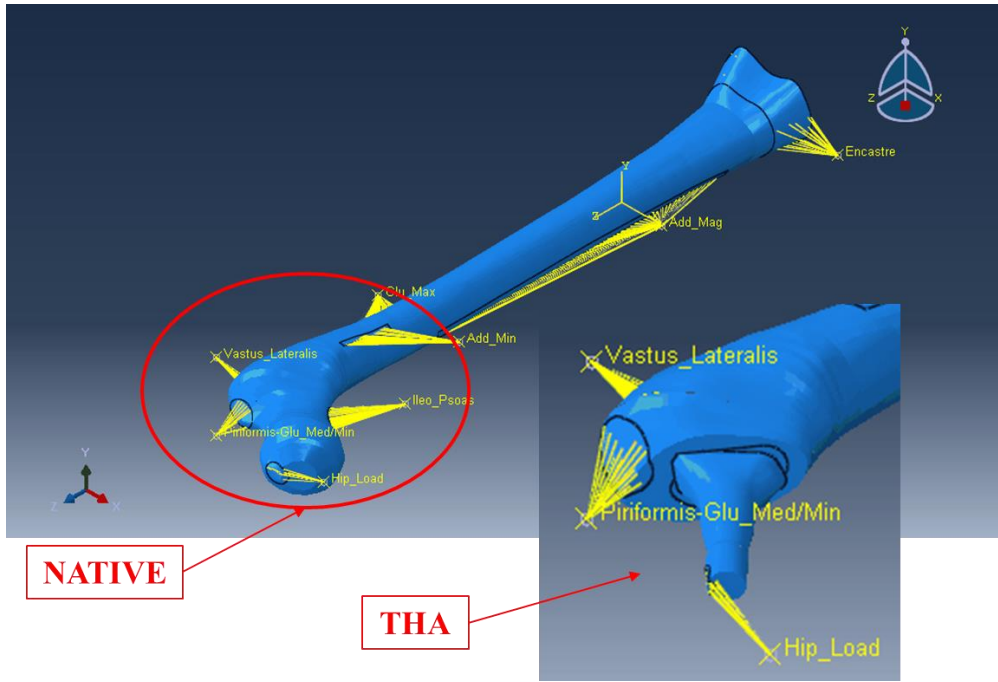


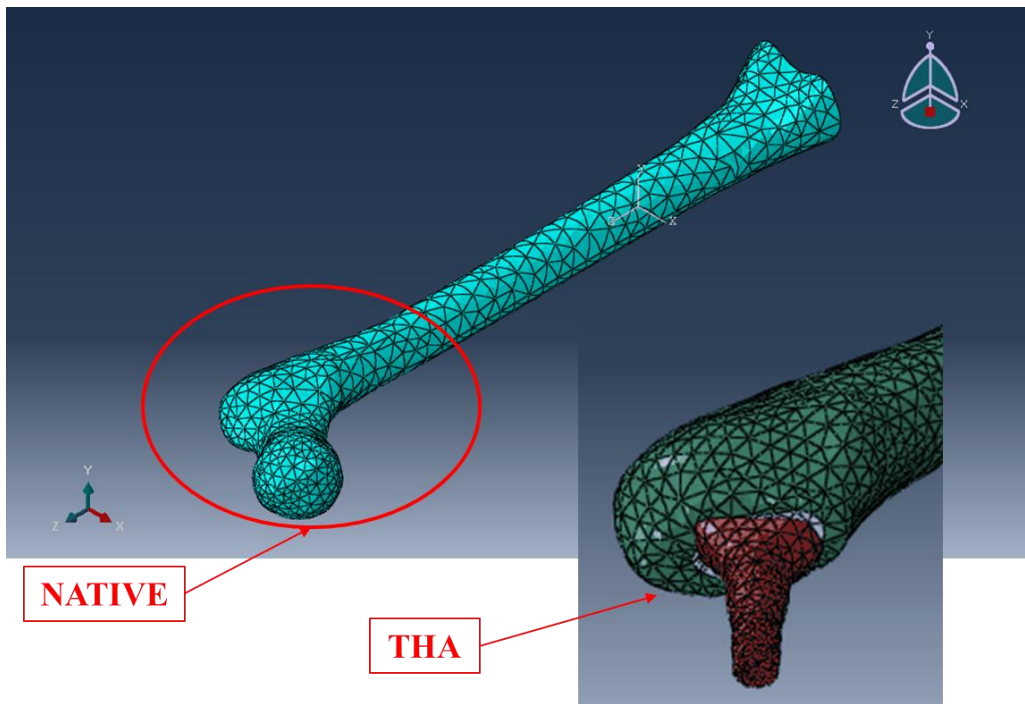
Figure 46: Flowchart of the interface with the addition of the possibility to add the prosthesis to the model.

In order to implant the prosthesis, first the femoral component of the prosthesis was properly positioned and the function *Cut* was used to simulate the osteotomy. The next step was to use the function *Merge* to connect the surface of the prosthesis with the one of the bone. The result, compared with the native femur is shown in Figure 47:





**.C**



**.D**



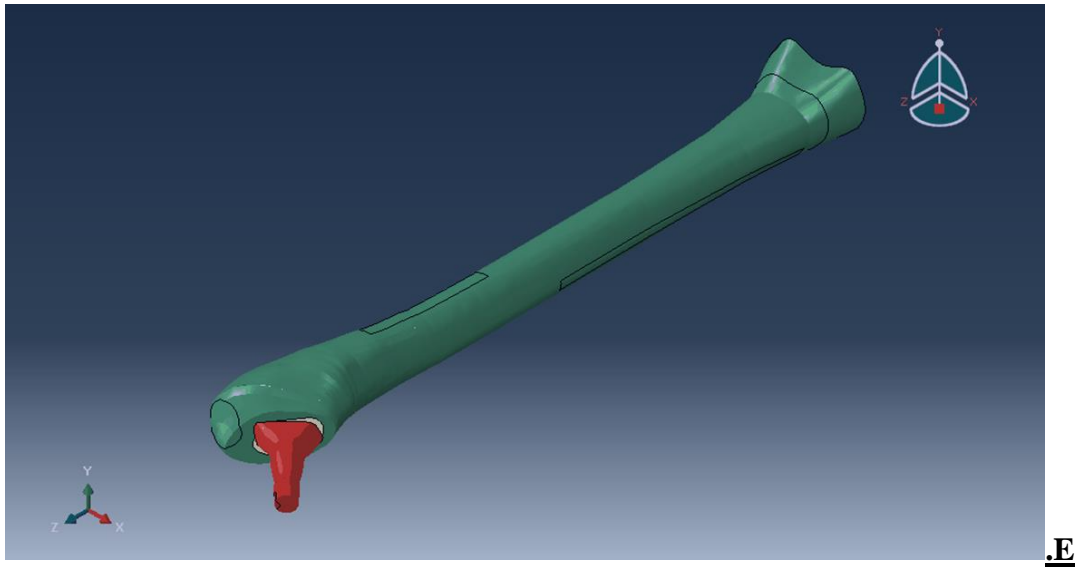


*Figure 47: Part realization (A), material (B), loads (C) and mesh (D) assignment, femur with prosthesis applied (E)*

### 4.3 Analytical Model

In order to validate the FE Model, the results, in term of stresses, have been compared to the ones obtained on an analytical model (Figure 48):

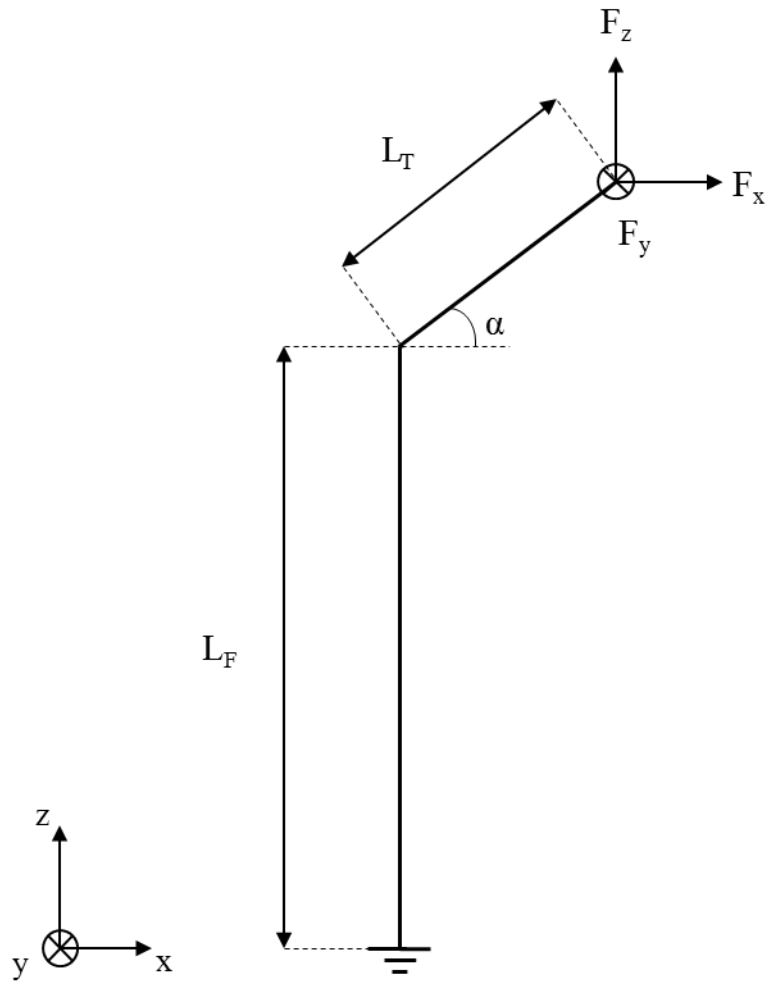
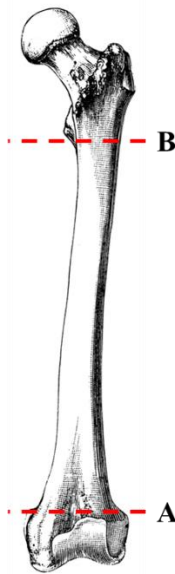


Figure 48: Representation of the analytical model.

In the model the following variables can be observed:

- $F_x$ ,  $F_y$  and  $F_z$ : are the three components in the main directions of the load acting on the femoral head;
- $L_T$ : is the length of the femoral neck;
- $\alpha$ : is the slope of the femoral neck respect the perpendicular to the stem;
- $L_F$ : is the femur's stem length, considering as extremes (Figure 49) the insertion point of the condyles with the femur (A) in the frontal plane and the beginning point of the small trochanter (B).

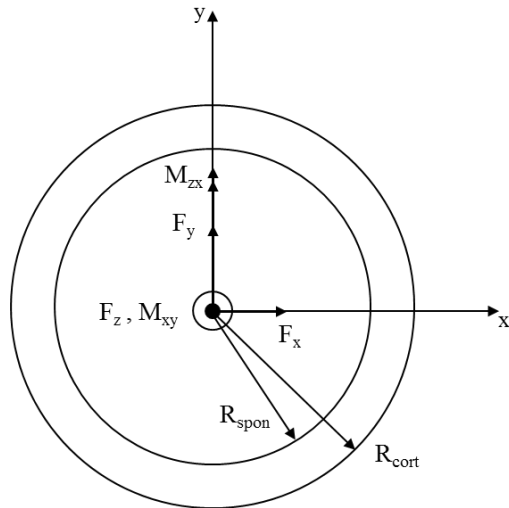


*Figure 49: Visualization of the extreme points to measure the femur's stem length.*

In order to calculate the stresses acting on the most stressed area, which is the femoral stem, the Saint-Venant's Problem was applied; as a consequence these assumptions were considered satisfied:

- No volume forces are acting on the solid;
- No surface forces are acting on the lateral surfaces of the solid;
- The material is homogeneous, elastic, linear and isotropic;
- No constraints are acting on the solid.

The femoral stem cross section, with the internal forces acting on it, can be represented as follows, assuming the approximation of it to a circular shape (Figure 50):



$$\begin{cases} M_{zx} = (L_F + L_T \sin \alpha) F_x - L_T \cos \alpha F_z \\ M_{xy} = L_T \cos \alpha F_y \end{cases}$$

Figure 50: Representation of the cross section, where  $R_{spon}$  and  $R_{cort}$  represent respectively the spongy and cortical radius.

The stress is determined by three main contributions:

$$\sigma = \sigma_{N,F} + \tau + \sigma_T;$$

where:

- $\sigma_{N,F}$  represents the contribution determined by the normal force and the bending moment;
- $\tau$  represents the contribution determined by the shear force;
- $\sigma_T$  represents the contribution determined by the torque moment.

#### 4.4 Output

In order to compare the stresses measured on model with different basic characteristics, seven regions have been identified following the model of Gruen (Figure 51), either with the application of the prosthesis or not.

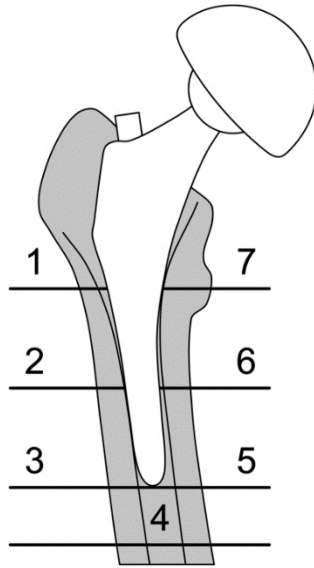


*Figure 51: Representation of the Gruen ROI (Region of Interest).*

To have a more accurate set of information, the seven ROI have been identified separately on the femur and the stem (in this case the fourth ROI does not appear since it is referred to the bone below the bottom of the prosthesis), and each of them has been divided in the anterior and posterior portions.

Moreover, in order to select the same elements for each ROI in different simulations, before running this last one, a Python file has been launched. Thanks to that, automatically a certain number of sets referring to each ROI is realized in Abaqus; in that way the elements for each region remain the same for different model, providing that no geometry modifications has been applied.

Lastly, the parameters chosen to compare the different simulations were the maximum Von Mises stress measured in that area for the prosthesis, and the maximal and minimal principal stresses for the femoral part.

## 5 RESULTS & CONCLUSION

### 5.1 Geometry Adaptation of the Model

The hypothesis previously introduced in the chapter regarding the modification of the default geometry (Ref. “4.2.1 Modification of the Geometry”) has been properly proved to be a legitimate assumption by manually calculating the angle of interest in the two following radiograph (Figure 52):

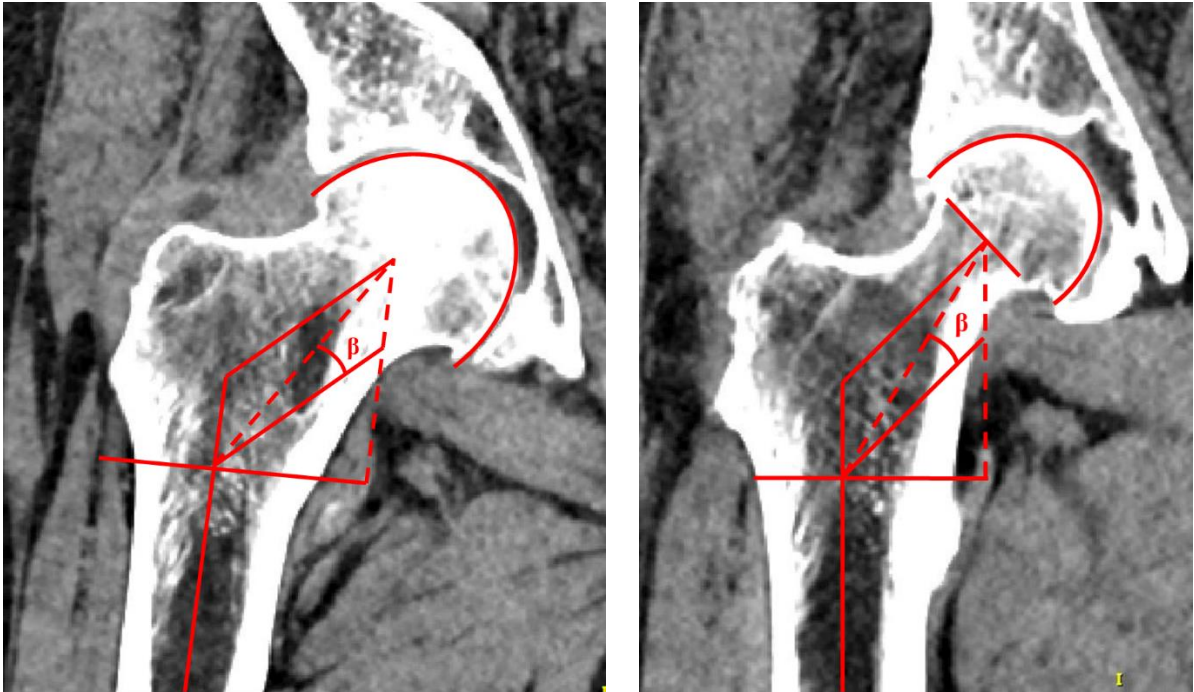


*Figure 52: Representation of the segments necessary to calculate the angle of interest.*

The results are reported in Table 4.

	<b>Radiograph 1</b>	<b>Radiograph 2</b>
<b><math>\beta</math></b>	14.862°	13
<b><math>\cos(\beta)</math></b>	0.96	0.97

*Table 4: Demonstration of the hypothesis accuracy.*

## 5.2 Validation of the Model

Concerning the validation of the model, this one was achieved in two different ways. First, the effectiveness of the parametric model was evaluated by a geometric point of view, which means that the default geometry was modified in order to obtain the one of a specific patient-. This was accomplished by using two radiographs of two different femurs (Figure 53).



Figure 53: Radiographs of the femur of two different patients.

The parameters of interest (Ref. 4.2.1 “Modification of Geometry”) were then calculated on these images and used to obtain the model in Abaqus (Table 5).

	<b>Radiography 1</b>	<b>Radiography 2</b>
<b><math>R_H</math> [mm]</b>	27.5	22
<b><math>\alpha</math></b>	47	50
<b><math>L_F</math></b>	330	304
<b><math>\gamma</math></b>	8	6.4
<b><math>I_\Phi</math></b>	30	20
<b>Thickness</b>	10	8

Table 5: Values of the parametes measured on the radiograph shown athe beginning of this chapter.



The comparison was qualitatively assessed, by comparing the model obtained in Abaqus with the original radiograph (Figure 54).

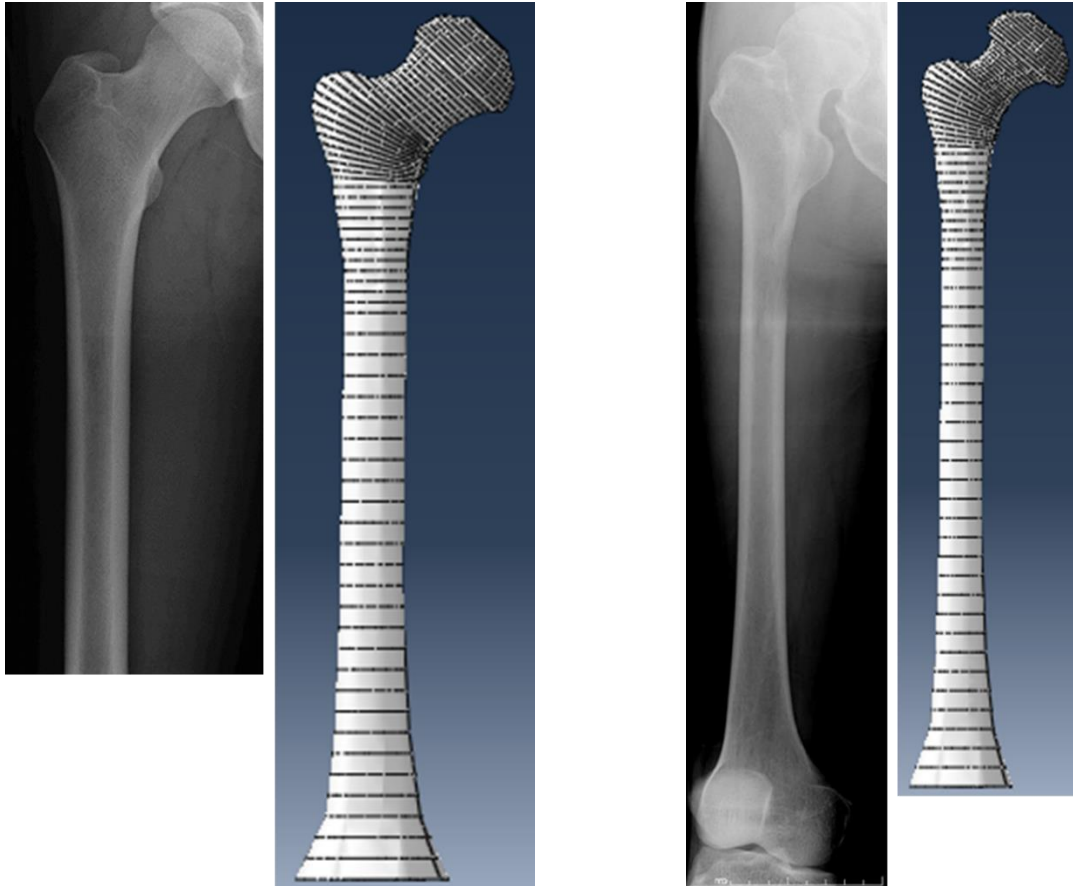


*Figure 54: Qualitative comparison of the radiographs with the models realized in Abaqus.*

The second way of validation assessed the reliability of the results. It was achieved by comparing the results obtained with the analytical model with those of the parametric finite element model. The femur model considered to attain the latter results was a healthy configuration, i.e. without the implantation of a prosthesis, as well it has not been considered in the analytical model.

The point of maximum sollecitation was located at the coordinates  $(R_{cort}, 0)$  (Figure 55).

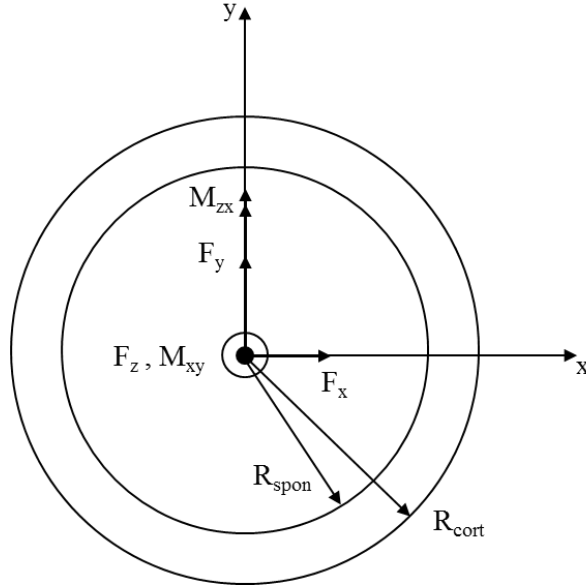


Figure 55: Representation of the cross section of the femoral stem at the isthmus level.

The contribution terms could then be expressed as below (traction gives a positive contribution):

$$\left\{ \begin{array}{l} \sigma_{N,F} = \frac{F_z}{A} - \frac{M_{zx}}{I} R_{cort}; \\ \tau = \frac{T * S}{I * b} = \begin{cases} \frac{R_y * S_x}{I * b_x} \\ \frac{R_x * S_y}{I * b_y} \end{cases}; \\ \sigma_T = \frac{M_T}{J} R_{cort} = \frac{M_{xy}}{J} R_{cort}; \end{array} \right.$$

where:

- Circular crown's area:  $A = \pi(R_{cort}^2 - R_{spon}^2)$ ;

- Moment of inertia:  $I = I_x = I_y = \pi \frac{(R_{cort}^4 - R_{spon}^4)}{4}$ ;
- Second moment of area:  $J = I_x + I_y = \pi \frac{(R_{cort}^4 - R_{spon}^4)}{2}$ ;
- First moment of area:  $\begin{cases} S_x = \iint_A y dA = \int_{R_{spon}}^{R_{cort}} \int_0^\pi r \sin \vartheta r d\vartheta dr; \\ S_y = \iint_A x dA = \int_{R_{spon}}^{R_{cort}} \int_{-\frac{\pi}{2}}^{\frac{\pi}{2}} r \cos \vartheta r d\vartheta dr; \end{cases}$
- Thickness of the cross section at the point considered:  $b_x, b_y$ .

By using the default geometry and as a load the one during the stance phase, the variables assumed the following values:

- $R_{cort} = 13.3$  [mm];
- $R_{spon} = 6.2$  [mm];
- $L_F = 330$  [mm];
- $L_T = 56$  [mm];
- $\alpha = 46$  [°];
- $F_x = 575.8$  [N];
- $F_y = -120.8$  [N];
- $F_z = -1947.12$  [N].

The point considered was subjected to a compression; the torque and shear contribution had no relevant effect, as shown in the results below:

$$\begin{cases} \sigma_{N,F} = -167.57 [MPa] \\ \tau = 0.256 [MPa] \\ \sigma_T = -1.50 [MPa] \end{cases}$$

The same process can be considered for the part of the femur which is subjected to traction; the point of maximum sollecitation (Figure ) in this case had coordinates  $(-R_{cort}, 0)$  and the resultant stress was the following:

$$\left\{ \begin{array}{l} \sigma_{N,F} = 159.10 \text{ [MPa]} \\ \tau = 0.256 \text{ [MPa]} \\ \sigma_T = -1.50 \text{ [MPa]} \end{array} \right.$$

Again, the torque and shear contributes were negligible in this case.

The predictions of the FE model, from which the muscles have been excluded in order to have a more accurate comparison since those are not included in the analytical model, are shown in Figure 56:

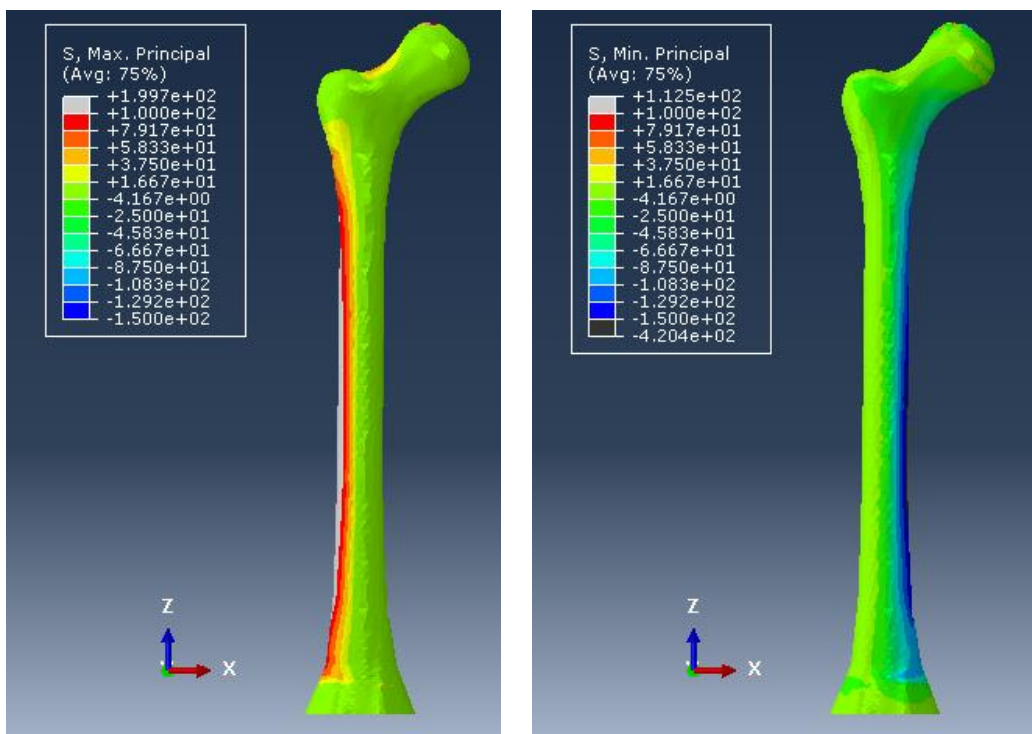


Figure 56: Maximum (left) and minimum (right) principal stresses ([MPa]) distribution on the femur.

By isolating the surface of interest in the two cases (Figure 57) it has been possible to calculate the maximum and minimum stress on that area, which correspond respectively to the maximum and minimum stress in traction and compression.

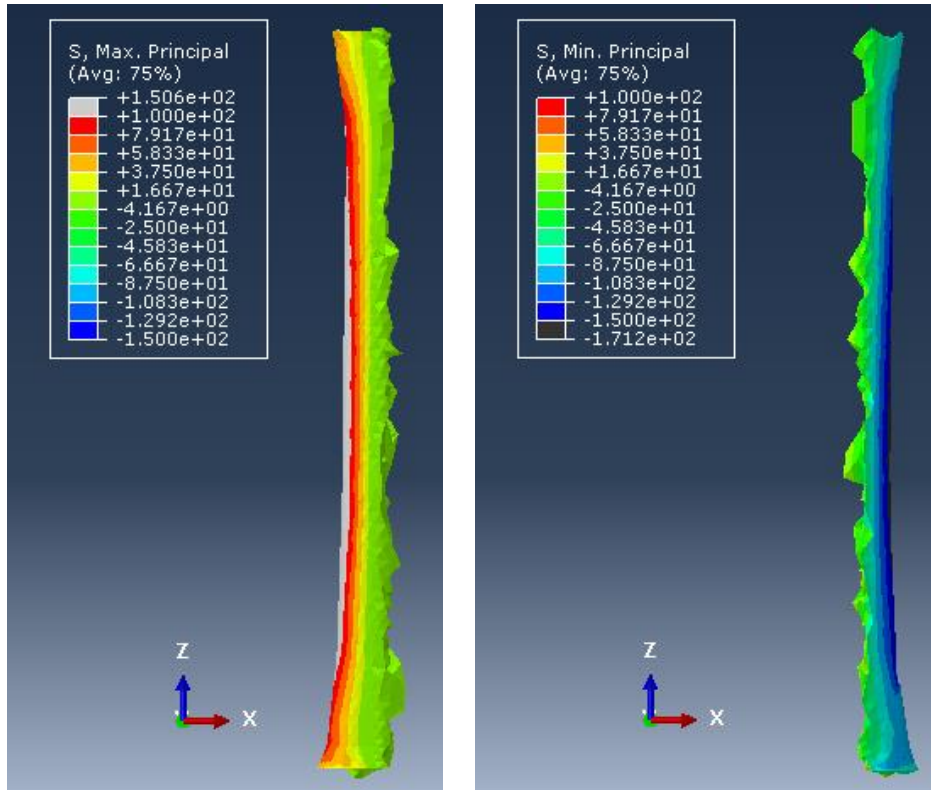


Figure 57: Surface subjected to traction (left) and compression (right)

The results were the following:

$$\begin{cases} \sigma_{Traction} = 150,6 [MPa] \\ \sigma_{Compression} = -171.2 [MPa] \end{cases}$$

The percentage differences between the results achieved on the analytical and FE model are reported in the Table 6 and it is possible to observe as their values are low and restrained.

	$\sigma_{\max, \text{princ}}$ [MPa]	$\sigma_{\min, \text{princ}}$ [MPa]
<b>FE Model</b>	150.6	-171.2
<b>Analitical Model</b>	159.10	-167.57
<b><u>Percentage Difference</u></b> [%]	<b>5.34</b>	<b>-2.1</b>

Table 6: Evaluation of the percentage difference between the results obtained on the analitical and FE model.

### 5.3 Comparison with the Gold Standard Model

During the realization of the parametric model, the function *Merge* has been used to assembly the femur and the prosthesis. Actually this is not best option to emulate the contact between the prosthesis and the bone, since it “fuses together” (unifies) the surfaces and give continuity to the displacement. For this reason a Gold Standard model has been realized, which has a *Tie* constraint, that fasten the two surfaces without fusing them together and reduce the effect of displacement continuity induced by the *Merge*, in order to compare the results with the parametric one and evaluate the entity of eventually differences.

The distribution of the stresses on the prosthesis in the two configuration is showed in Figure 58:

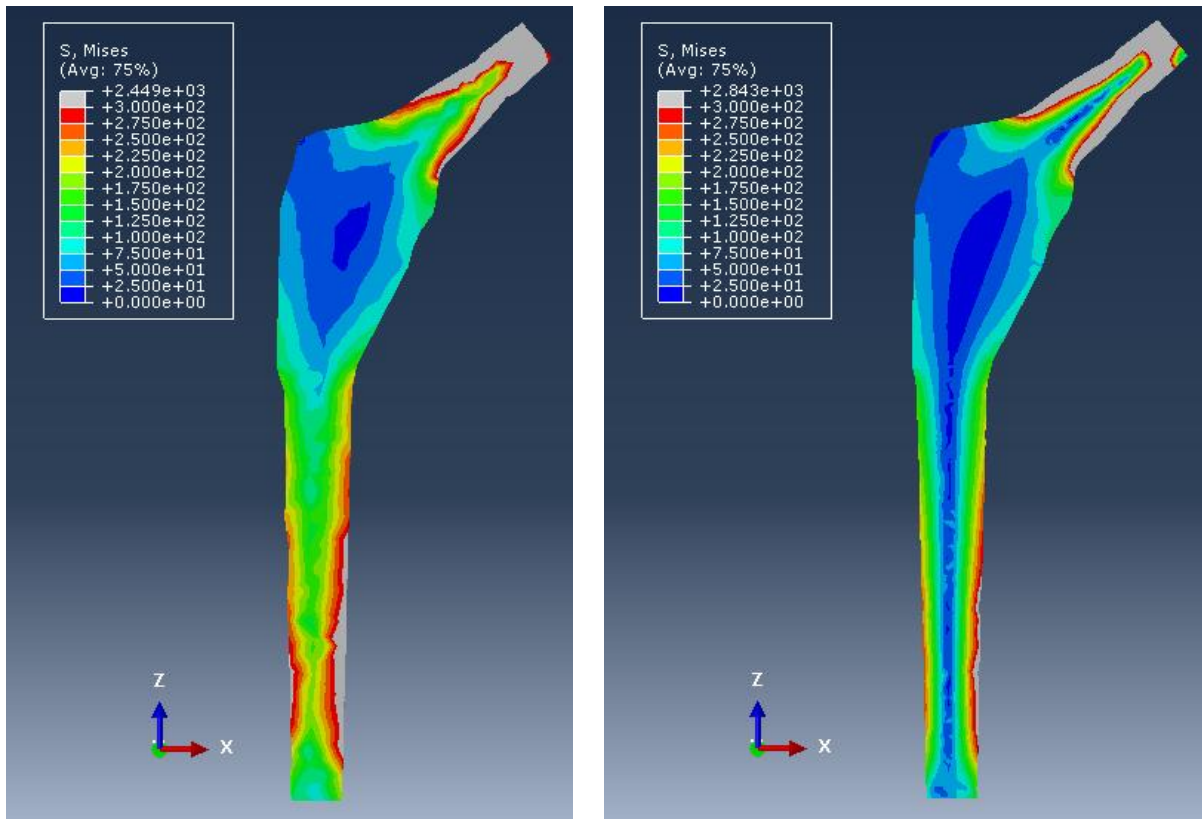
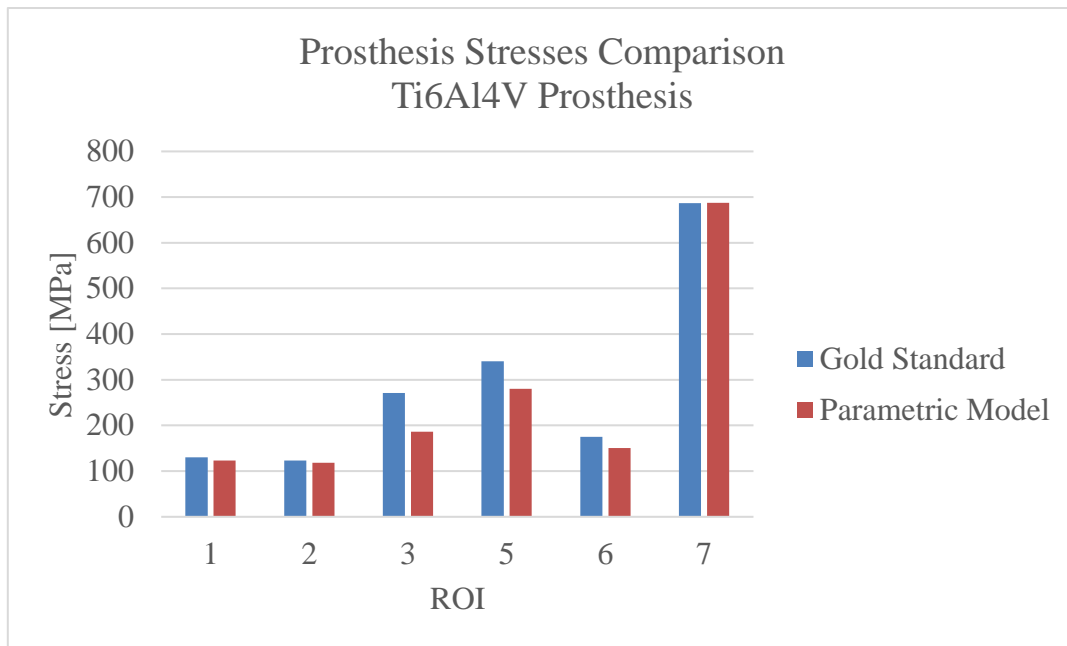


Figure 58: Stresses distribution on the prosthesis in the gold standard (left) and parametric model (right)

The maximum stress, in term of Von Mises stress, measured in each ROI in the two cases is shown in the histogram below (Figure 59).



*Figure 59: Maximum Von Mises stress measured on the prosthesis in each ROI, either with the gold standard and parametric model.*

The same process can be applied to the femoral part. The distribution of the stresses is shown below (Figure 60, 61):



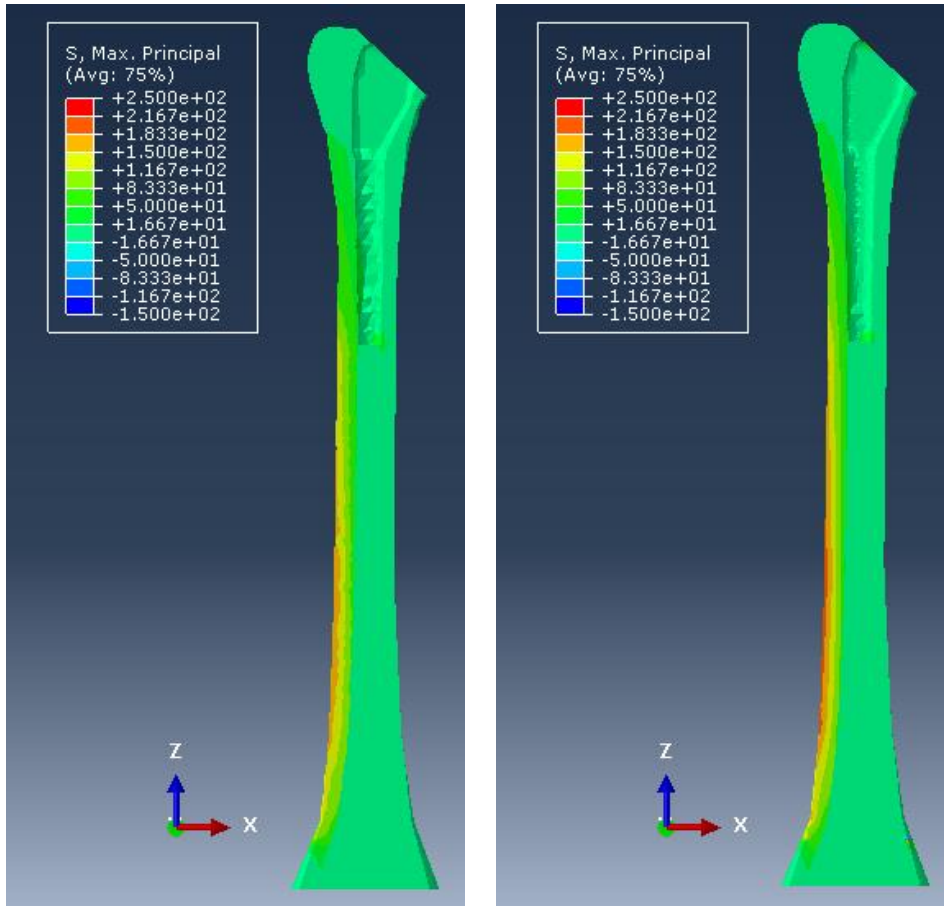
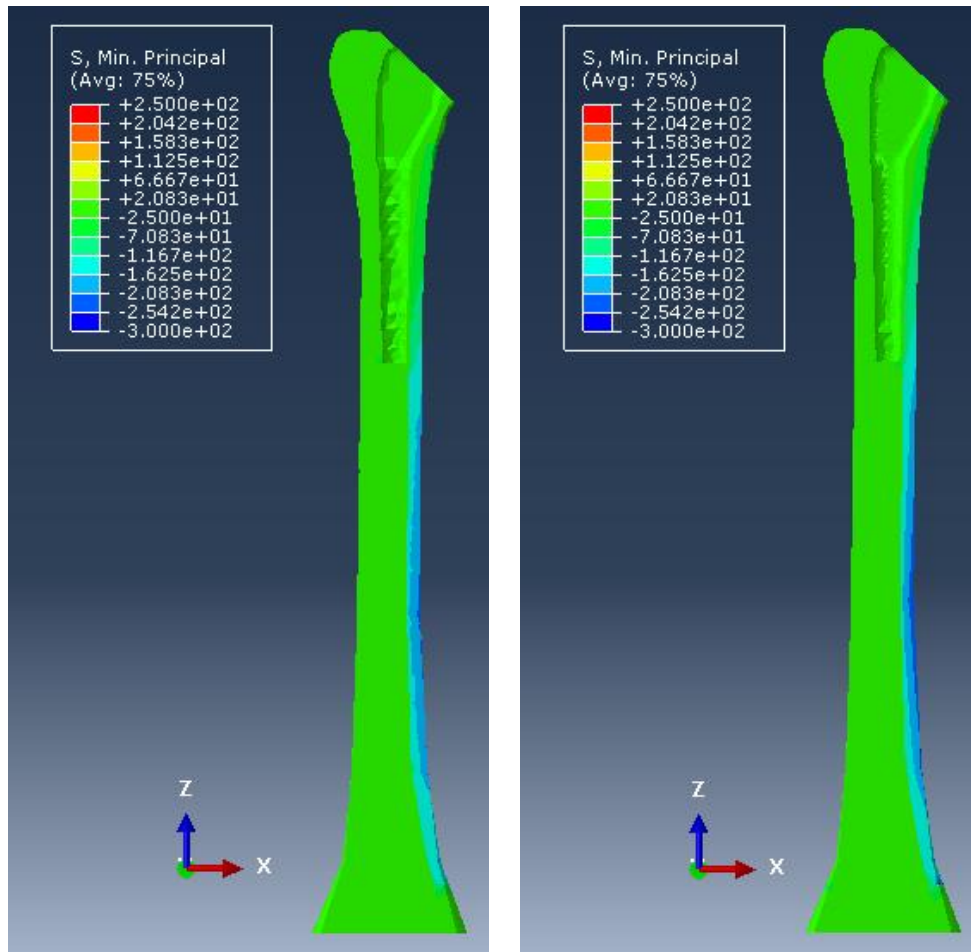


Figure 60: Maximum principal stresses ([MPa]) distribution on the femur in the gold standard (left) and parametric (right) model.



*Figure 61: Minimums (second two images) principal stresses ([MPa]) distribution on the femur in the gold standard (left) and parametric (right) model.*

The maximum/ minimum stress value measured in each ROI are reported in the following histogram, in term of maximum and minimum principal stress (Figure 62, 63)

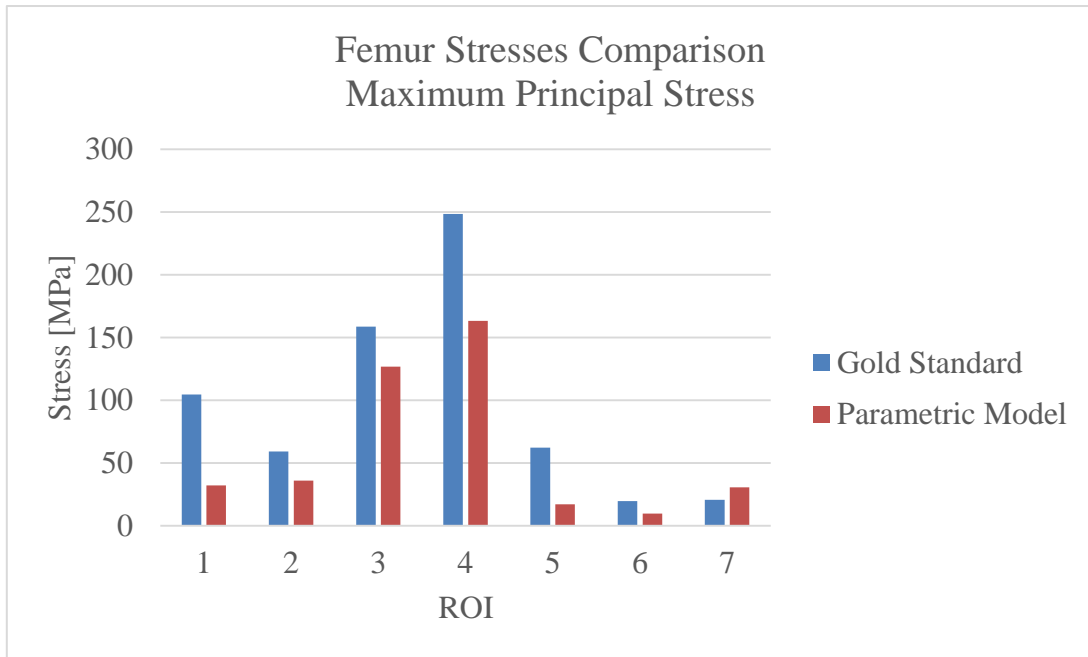


Figure 62: Comparison between the gold standard and parametric model in term of maximum principal stress on the bone in each ROI.

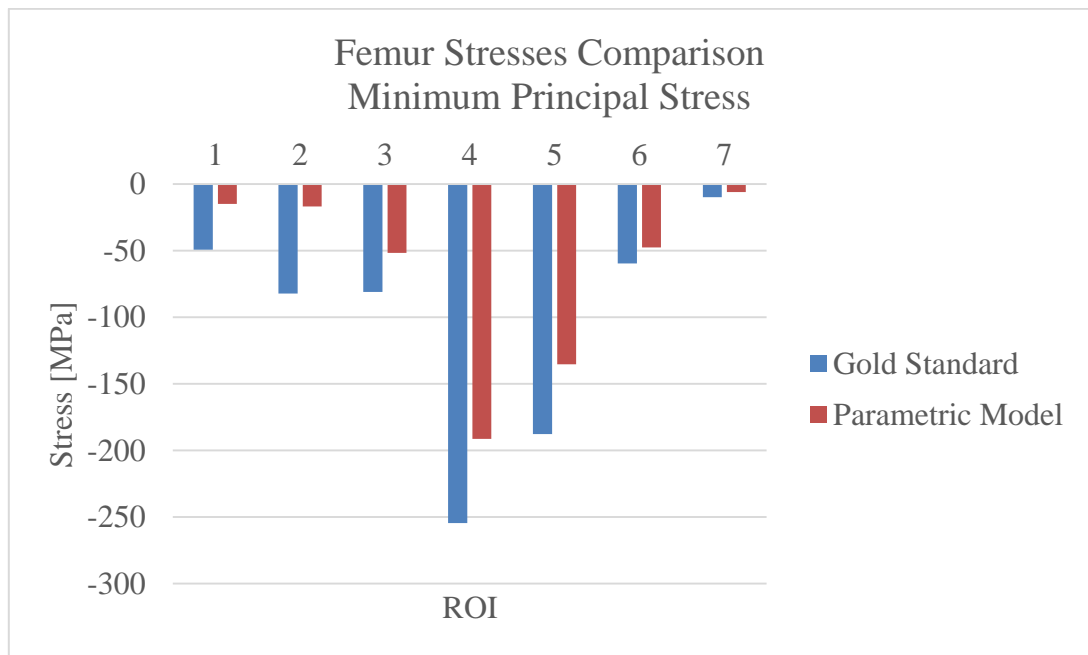


Figure 63: Comparison between the gold standard and parametric model in term of minimum principal stress on the bone in each ROI.

It is possible to observe in the first 4 ROI a significative difference between the values measured on the gold standard and parametric model; those can be either induced by the presence of muscles in that area or by selecting a different number of elements in the two model, which can implies isolating element subjected to higher stresses. This topic is discussed more in details forward in the study (*Ref “5.5 Discussion & Conclusion”*).

## 5.4 General Simulation

Different simulations have been conducted using the model realized; some examples are reported in this chapter.

First, the effect of using prostheses with different mechanical properties has been investigated. In particular the stresses distribution on the femur with a Ti6Al4V and CoCrMo prostheses has been studied, and compared to the ones acting on a healthy femur (no prosthesis implanted). The histograms of the maximum and minimum principal stresses in the ROI of interest are shown below (Figure 64, 65).

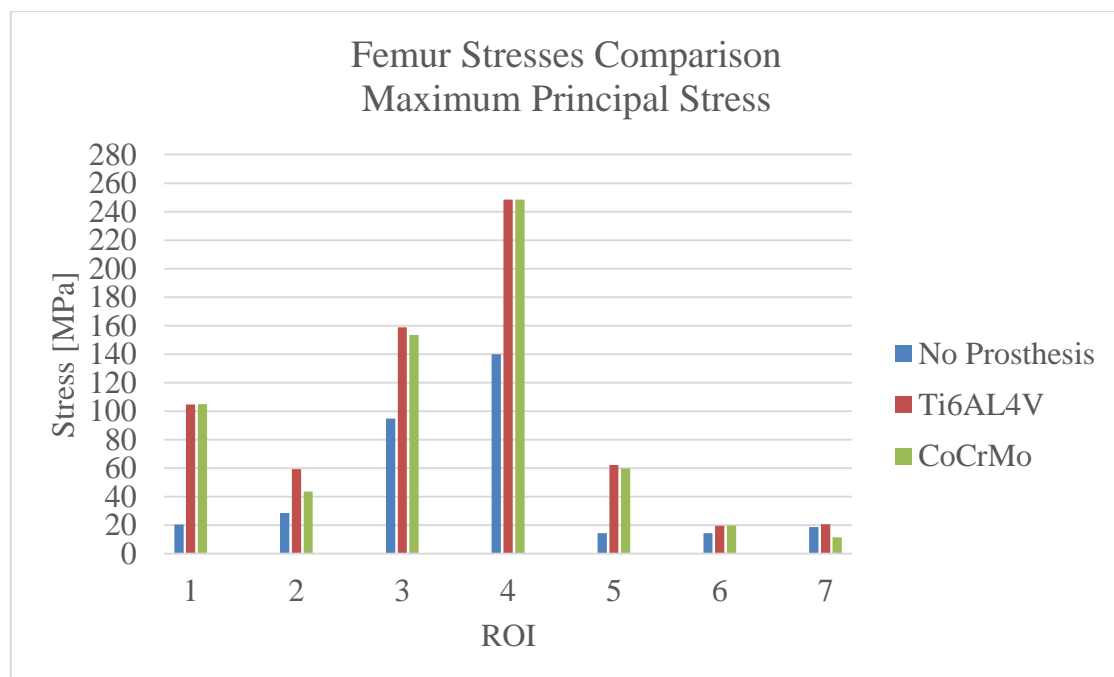


*Figure 64: Comparison between the femur with no prosthesis applied, gold standard and parametric model in term of maximum principal stress on the bone in each ROI.*

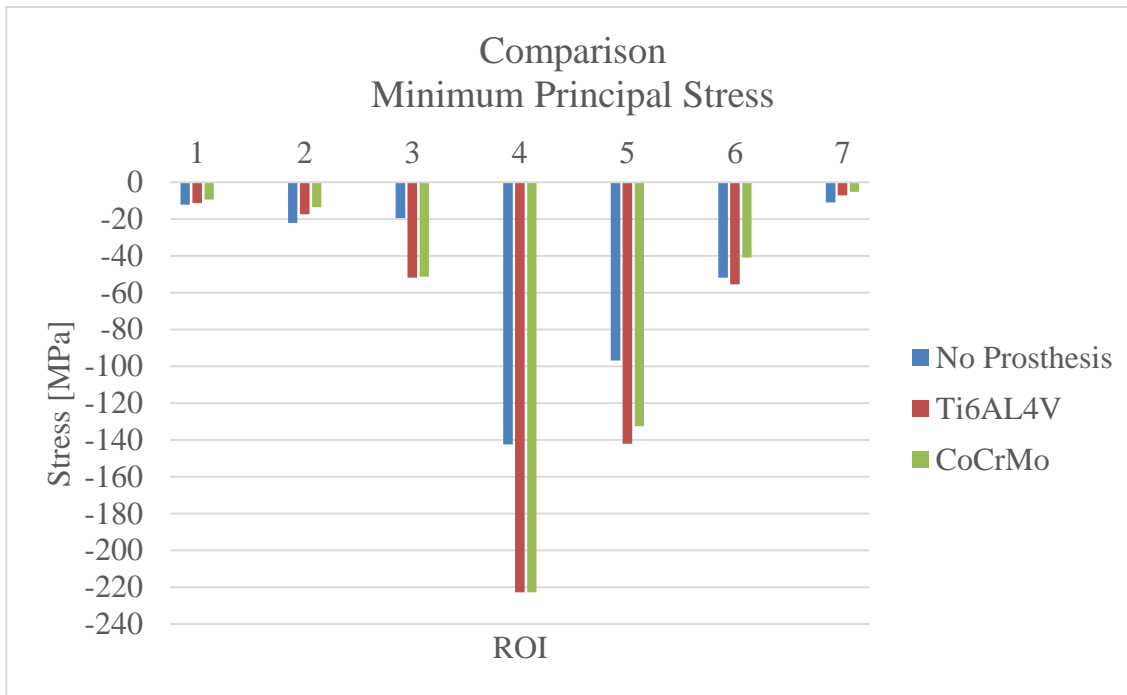


*Figure 65: Comparison between the femur with no prosthesis applied, gold standard and parametric model in term of minimum principal stress on the bone in each ROI.*

The effect of varying the Young's Modulus of the femur has also been investigated. To this aim, Young's Moduli referred to a physiologic, osteopenic and osteoporotic femur have been used and the results, in terms of maximum and minimum principal strains, have been compared. The distribution of those is shown in the Figures below (Figure 66, 67).

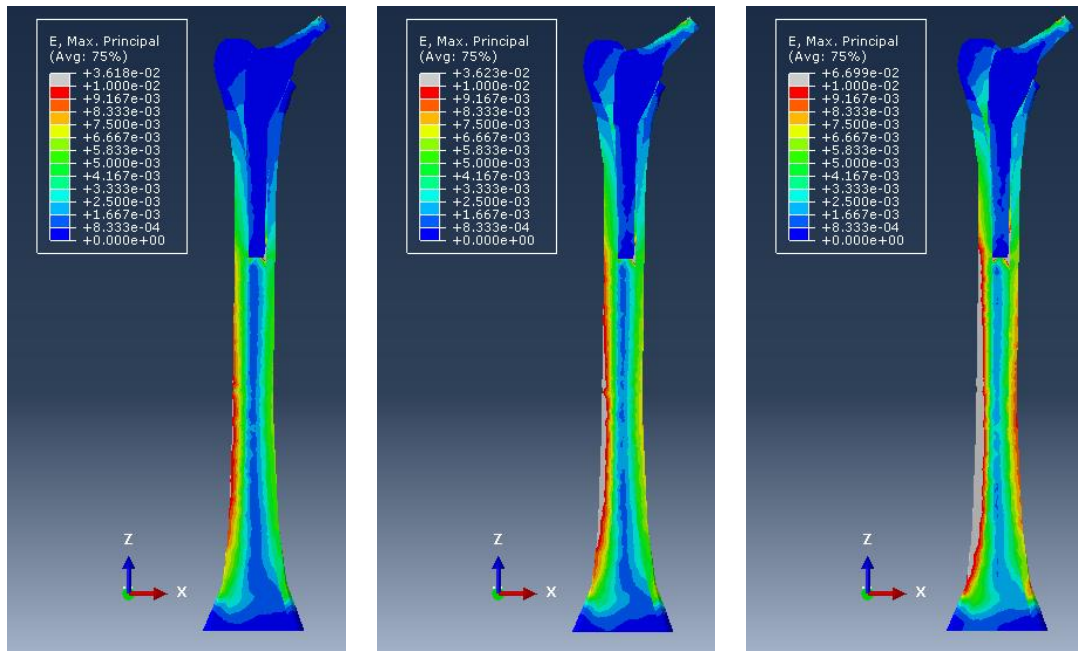


Figure 66: Maximum principal strains distribution on a healthy (left), osteopenic (center) and osteoporotic (right) femur with prosthesis applied.

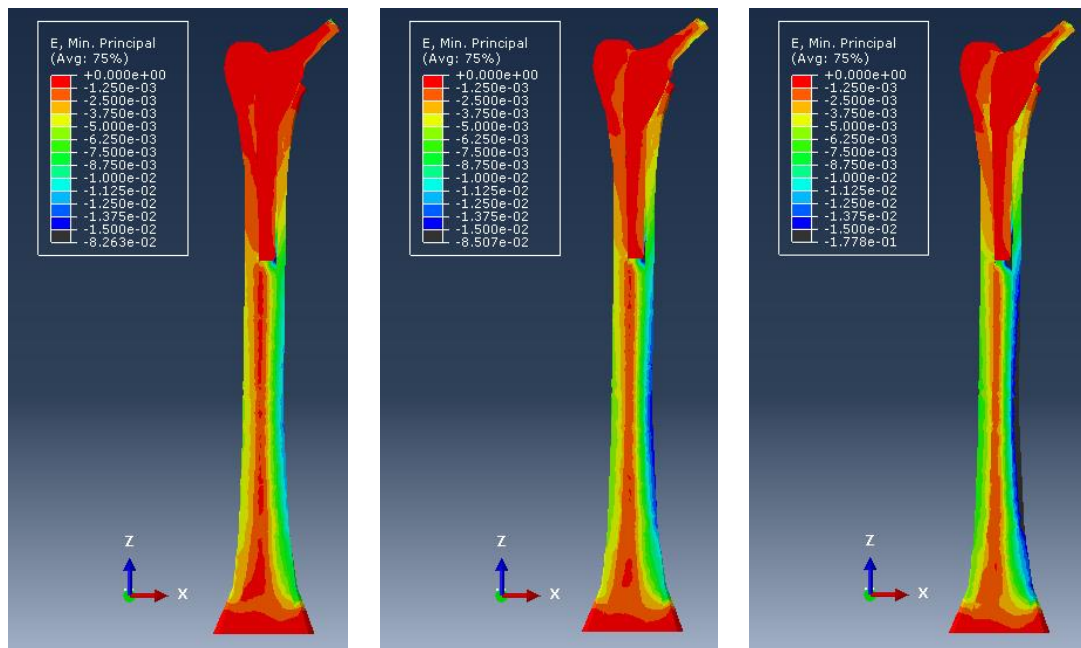
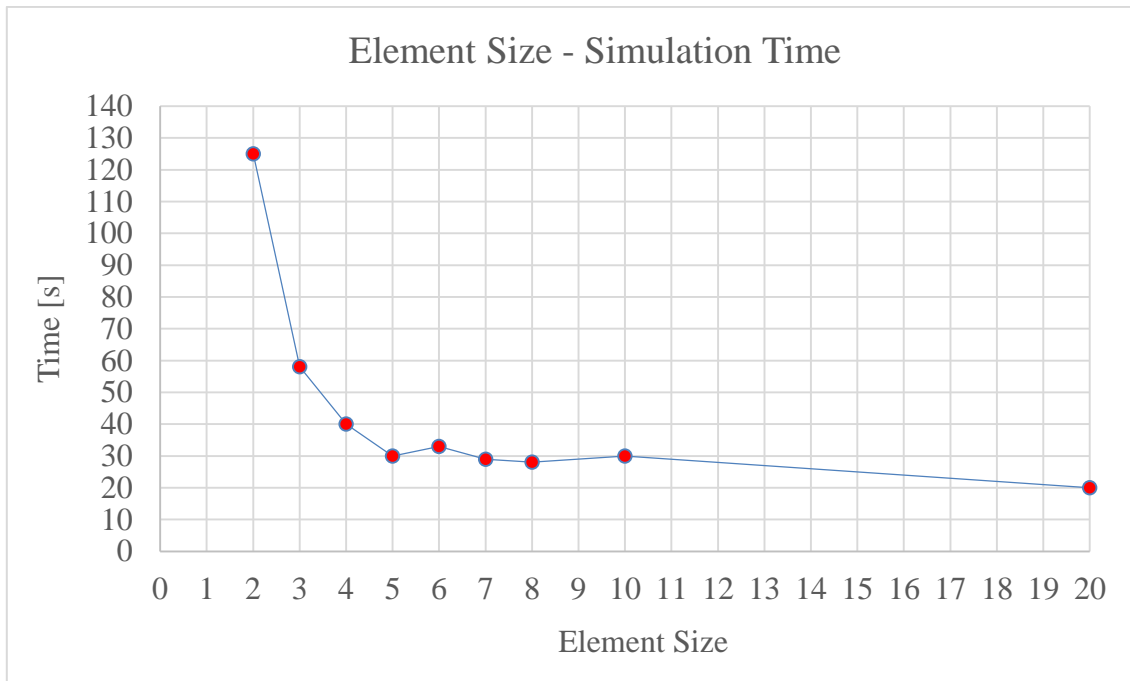


Figure 67: Minimum principal strains distribution on a healthy (left), osteopenic (center) and osteoporotic (right) femur with prosthesis applied.

## 5.5 Simulation's Speed & Number of Elements

The model had a suitable simulation's speed. Indeed, the required times to perform the simulations have been calculated for various element sizes of the mesh (Figure 68).



*Figure 68: Relation between the variation of the element size of the mesh and the time necessary to complete the simulation.*

The reason why the values measured are particularly low is connected to the number of elements generated on the model, which is indeed not too high (Figure 69).

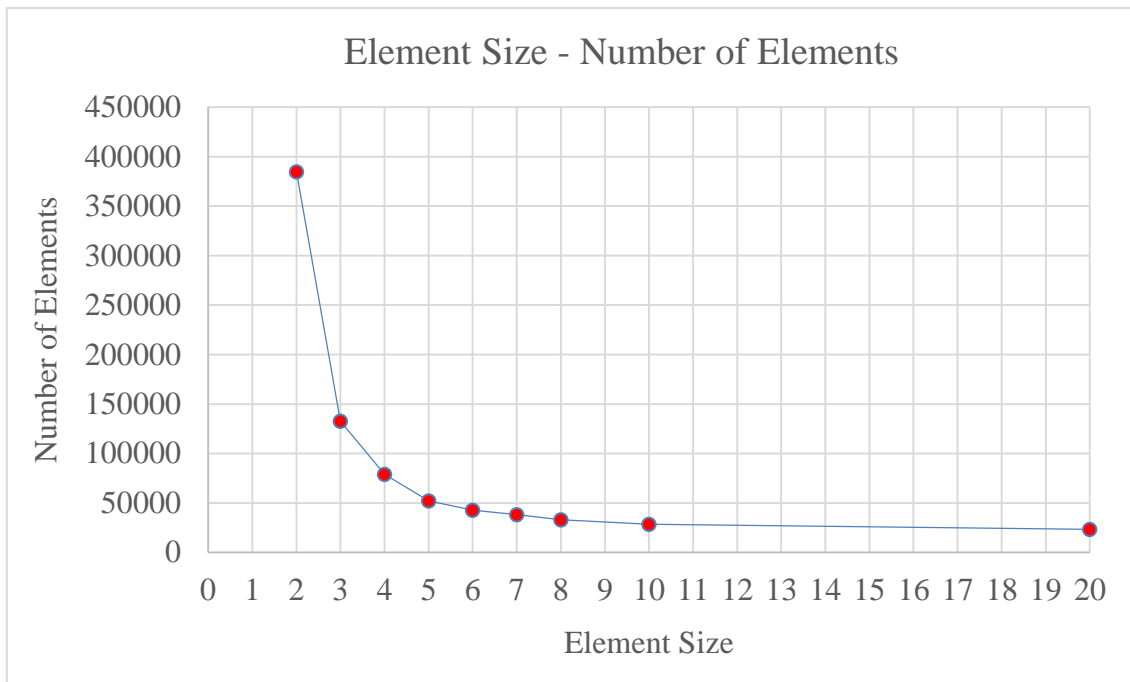


Figure 69: Relation between the variation of the element size of the mesh and the number of elements generated on the model.

## 5.6 Discussion & Conclusion

By optically comparing the radiographs of the femur and the FE model obtained by using the parameters measured on that one it is possible to observe an high similarity of these two; this demonstrate that the coefficients realized and used to obtain the femoral geometry of a specific patient allowed for a properly customization of the default one.

The percentage differences detected between the analytical and FE model are mostly related to:

- Geometrical simplifications and approximations applied to the analytical one (*Ref. 4.3 “Analytical Model”*), such as considering the cross section circular and the measurement of the parameters of interest;
- Considering the load acting on the analitical model not distributed on a certain surface, as it is for the FE model.

However, the results show that the the percentage differences have a low and restrained value, which means the FE model is efficient and accurate.



The comparison between the femoral stresses distribution on the Gold Standard and parametric model has shown some higher values in the first one; actually this is not indicative of errors present in the parametric model and there are two main reasons to explain these differences, which are the following:

- The elements considered in Abaqus to extract the stresses in the area of interest are selected manually, so there is the possibility to realize a wider or narrower area. This implies that a part of a region with higher stresses could be selected or not in one of the two model while in the other one not;
- On the anterior part of the trochanteric region the vastus lateralis muscle is acting, which contribution is not negligible in particular in the first two ROI, as shown in the histograms below (Figure 70)

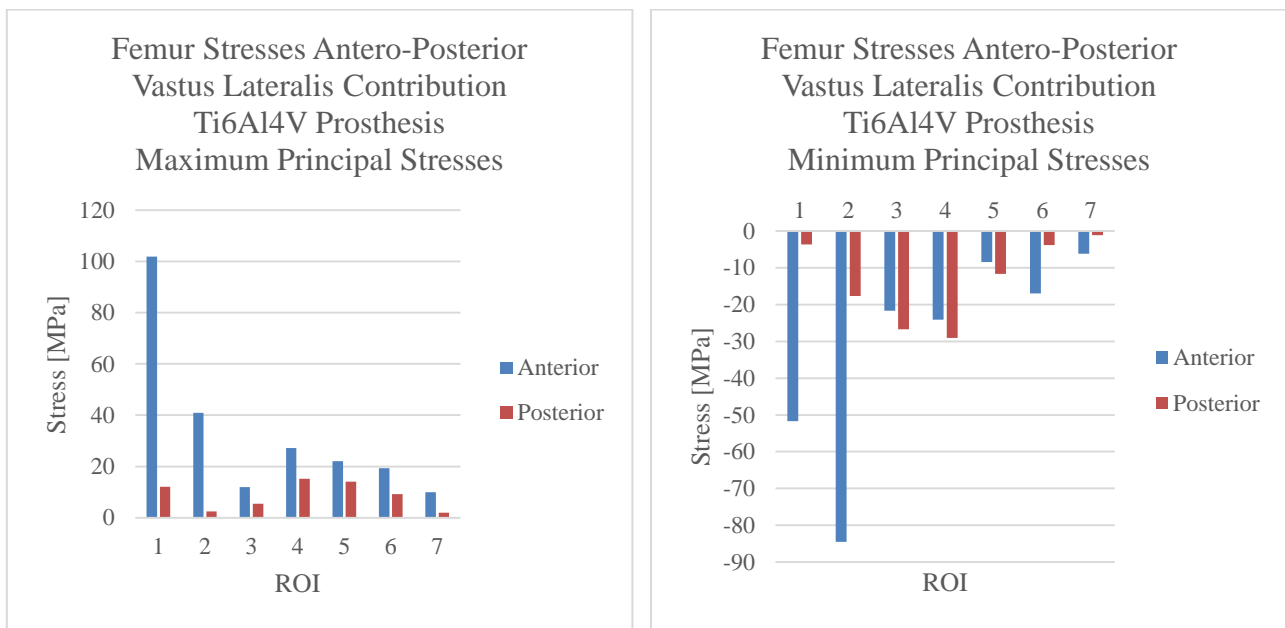
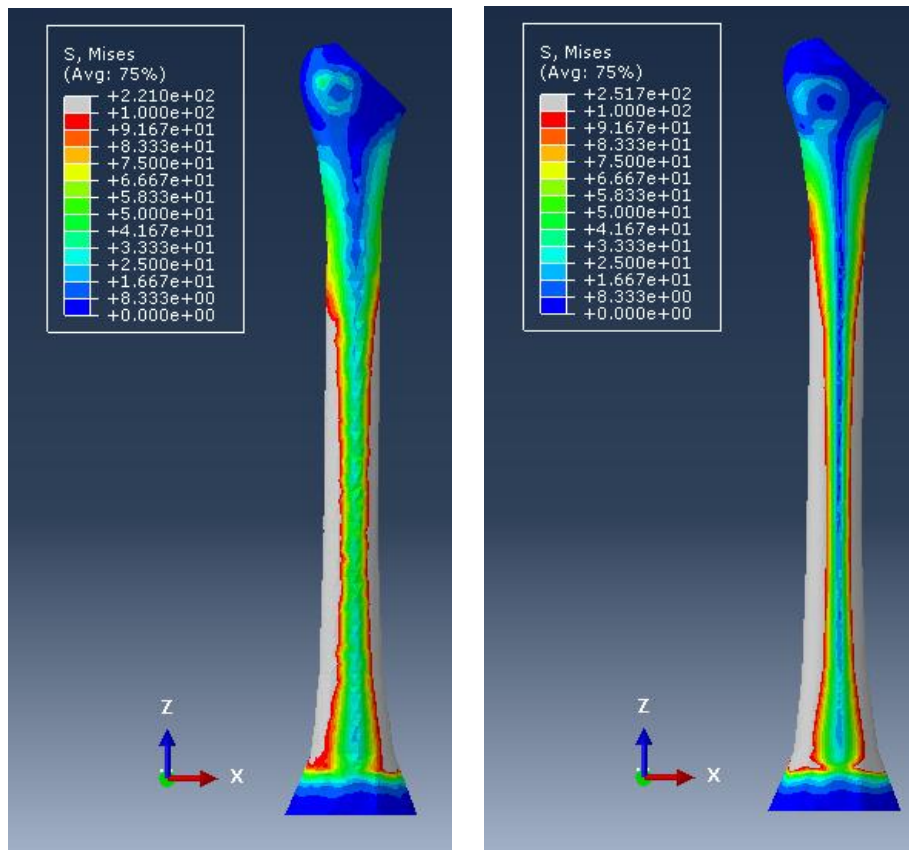


Figure 70: Maximum (left) and minimum (right) principal stress in the anterior and posterior plane on the bone in each ROI induced by the presence of the vastus lateralis muscle.

However, the insertion area on the two models is slightly shifted; indeed, as shown in Figure 71, in the parametric model this area is placed lower than the one in the gold standard and it is positioned in a region with higher stresses, so the contribution of the muscle is less relevant.



*Figure 71:Stresses distribution in the gold standard and parametric model.*

Moreover, by calculating the stresses in the anterior and posterior plane in the gold standard model, by neglecting the values on the anterior part (since the major contribution in the first two ROI is determined by the presence of the vastus lateralis muscle), it is possible to notice similarity of the values measured on the parametric model. The histograms, with the stresses values, are reported below (Figure 72, 73).

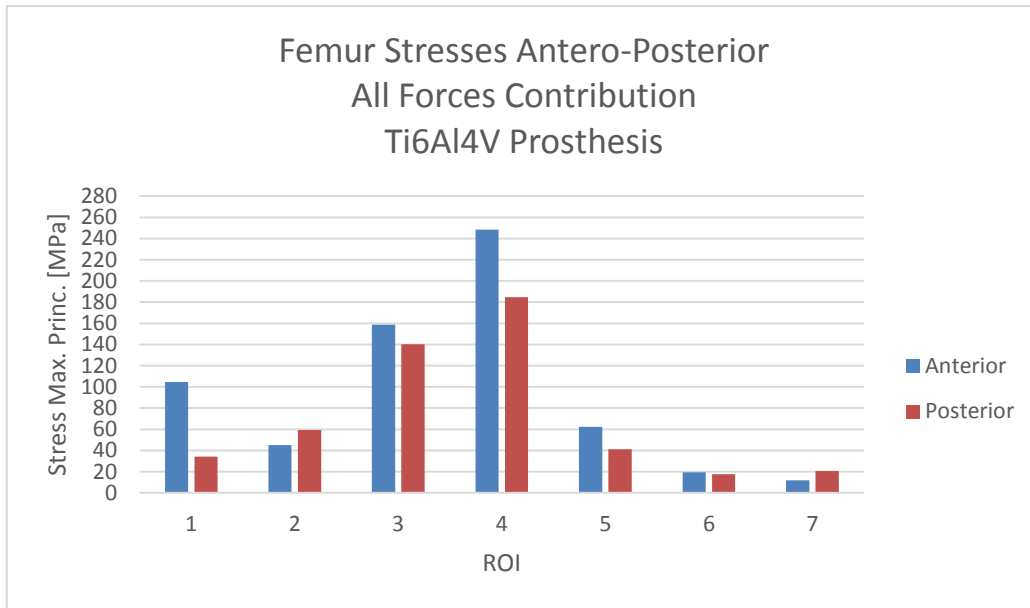


Figure 72: Maximum principal stress in the anterior and posterior plane on the bone in each ROI on the gold standard model.

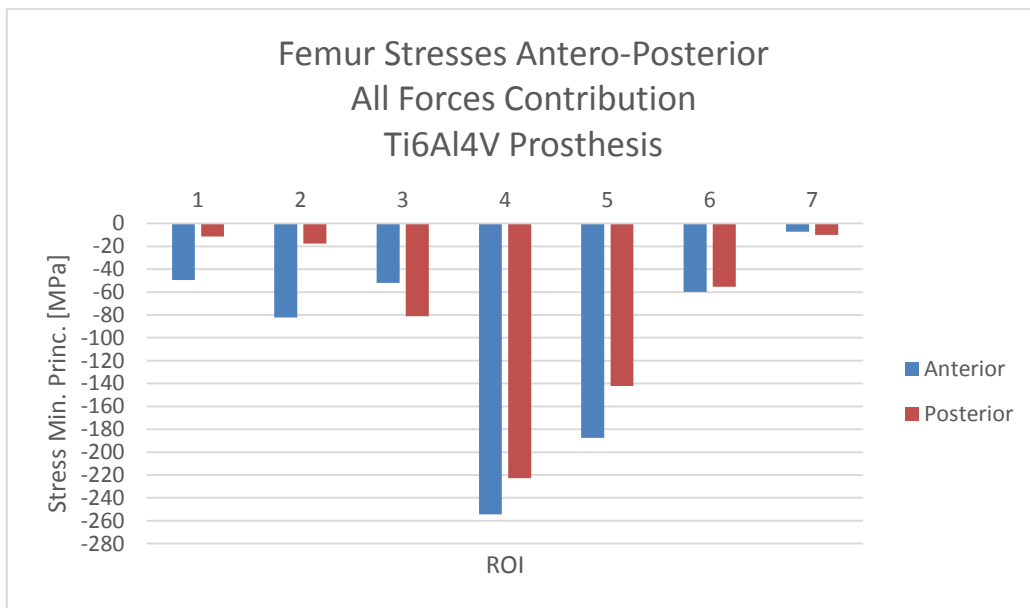


Figure 73: Minimum principal stress in the anterior and posterior plane on the bone in each ROI on the gold standard model.

Therefore the function *Merge*, which does not exactly replicate the real interaction between the prosthesis and femur surface, has not shown any significant differences in terms of stress

distribution. Actually, the two function, *Merge* and *Tie*, are pretty similar conceptually and in terms of displacement continuity; the only difference is in their definition, since the first one unifies the surfaces while the second one ties them together. The properly interaction that has should be used is the one defined by the function *Surface-To-Surface*, which allows to define the friction coefficient. However, by applying this one to the model, the software Abaqus has not been able to conclude the simulation even by giving very long time of simulation. So due this reason and also because the micromovements at the interface are very limited, the function *Tie* has been considered acceptable.

In conclusion, it is then possible to affirm that the model realized is reliable and efficient; the simulation's times are restrained, with a low number of elements generated on the model, characteristic which moreover do not affect the precision and accuracy of the FE model realized (*Ref. "5.5 Simulation's Speed & Number of Elements"*).

## 6 FUTURE DEVELOPMENTS

The most important development regarding this project could be the parametrization of the prosthetic component, using a procedure similar to the one applied on the femur. The purpose of this process would be to allow the user to manage the prosthesis:

- Geometry;
- Material (which is actually already been implemented);
- Position respect the femur.

In order to accomplish this, the parameter requested could be:

- The slope of the prosthesis respect the frontal, transversal and sagittal plane;
- The prosthesis stem's length, as well the width and the thickness.

By realizing this, it would be possible to simulate and study the effect of different prosthesis design and positionings into the femur.

However, by implementing also this option, the simulation time would extend in a way not yet examined; in conclusion, it would be first necessary to evaluate how much this factor would increase and if the software Abaqus is the best option to achieve this goal.

Another interesting development would be to compare the results achieved in this study with others published in other works; actually this could be a difficult task since in most of the study it is not possible to obtain the parameters of interest from the radiographic images necessary to realize the parametric model. So, alternatively, FE model already validated, from which the parameters are easily measurable, could be used to fulfill the numerical validation.

## 7 BIBLIOGRAPHY

- [1] <http://medicinapertutti.altervista.org/argomento/articolazione-dellanca-o-coxo-femorale/>;  
11/08/2016.
- [2] Force Actions Transmitted by Joints in the Human Body. J.P. Paul; *Proc. R. Soc. Lond.*  
(1976), 163-172.
- [3] F. Franchin; *La Protesi d'Anca di Primo Impianto* (2003).
- [4] T. Villa, R. Pietrabissa; *Corso di Endoprotesi* (2013).
- [5] Biomechanics for Hip Arthroplasty. M. M. Morlock et al.; *Assessment* (2011), 159-168
- [6] Polyethylene Wear and Osteolysis Is Associated With High Revision Rate of a Small Sized  
Porous Coated THA in Patients With Hip Dysplasia. P. J. Murray et al.; *The Journal of  
Arthroplasty* (2014), Vol.29:1373-1377.
- [7] G. Pennati; *Corso di Costruzioni Biomeccaniche* (2015).
- [8] S. Farè, R. Chiesa; *Corso di Biomateriali* (2015).
- [9] Le Protesi di Ginocchio di Primo Impianto. U. De Nicola, N. Pace; *Springer* (2005), 245-246.
- [10] Mechanical, Anatomical, and Kinematic Axis in TKA: Concepts and Practical Applications.  
J. J. Cherian et al.; *Springer* (2014), Vol.7:89-95.
- [11] Principles of CT and CT Technology. L.W. Goldman; *J Nucl Med Technol* (2007);  
Vol.35:115–128.
- [12] Bernardo Innocenti; *Medical Devices Course*.

- [13] Basic Science Considerations in Primary Total Hip Replacement Arthroplasty. S.B. Mirza et al; *The Open Orthopaedics Journal* (2010), Vol.4:169-180.
- [14] <http://orthoload.com/test-loads/standardized-loads-acting-at-hip-implants/>; 30/10/2016
- [15] Analisi Numerica dell'Evoluzione Morfologica di un Femore sotto l'Azione di Carichi Fisiologici. M. Fredducci et al; *Tesi di Dottorato* (2006).
- [16] <http://www.arthroscopichipsurgeon.com/hip-arthroscopy.html>; 28/03/2017
- [17] <http://www.webmd.com/osteoarthritis/guide/hip-osteoarthritis-degenerative-arthritis-hip#1>; 18/03/2017
- [18] <http://www.protesiginocchioanca.com/protesi-anca.htm>; 28/03/2017
- [19] [http://www.webmd.com/rheumatoid-arthritis/guide/hip-rheumatoid\\_arthritis#1](http://www.webmd.com/rheumatoid-arthritis/guide/hip-rheumatoid_arthritis#1); 28/03/2017
- [20] Kinesiology of the Hip: A focus on Muscular Actions. D. A. Neumann; *Journal of Orthopaedic Sports Physical Therapy* (2010), Vol.40 (2):82-94.
- [21] Traumatic Hip Dislocation. S. Sanders et al; *Bulletin of the NYU Hospital for Joint Diseases* (2010), Vol.68 (2):91-96.
- [22] F. Migliavacca. *Corso di Biomeccanica* (2012).
- [23] Titanium Implants Induce Expression of Metalloproteinases in Bone during Osseointegration. V.I. Shubayev; *Journal of Rehabilitation Research & Development* (2004); Vol.41 (6A):757-766.
- [24] Bearing Surfaces in Hip Replacement - Evolution and Likely Future. N. Kumaret al; *Med. J. Armed Forces India* (2014), vol.70 (4):371–376.
- [25] Femoral Head Diameter Considerations for Primary Total Hip Arthroplasty. J. Girard; *Orthopaedics & Traumatology: Surgery & Research* (2015), Vol. 101 (1): 25–9.
- [26] <http://www.gkqcw.com/gkwinclude/show.asp?id=162>; 29/03/2017

- [27] Periprosthetic Fractures Associated with Osteolysis: a Problem on the Rise. D. J. Berry; *The Journal of Arthroplasty* (2003), Vol. 18 (3):107–111.
- [28] <http://www.mydepuhiprecall.com/2013/05/the-depuy-hip-litigation-guide.html>; 29/03/2017
- [29] Cemented versus Uncemented Fixation in Total Hip Replacement: a Systematic Review and Meta-analysis of Randomized Controlled Trials. A. Abdulkarim et al.; *Orthopedic Reviews* (2013), Vol.5:34-44.
- [30] Assessment of the Proximal Femoral Morphology Using Plain Radiograph-Can it Predict the Bone Quality?. Y. Yeung et al.; *Journal of Arthroplasty* (2006), Vol.21 (4):508-513.
- [31] The Effect of Aging on the Shape of the Proximal Femur. Noble PC. et al.; *Clin. Orthop. Relat. Res.* (1995), 31:44.
- [32] Anatomy of the Proximal Femoral Medullary Canal and Fit and Fill Characteristics of Cementless Endoprosthetic Stems. H. Laine; *Acta Universitatis Tamperensis* 797 (2001).
- [33] Comparison of Stress Shielding between Straight and Curved Stems in Cementless Total Hip Arthroplasty – An in Vitro Experimental Study. C. Tai et al.; *Journal of Medical and Biological Engineering* (2004), Vol.24 (4):177-181.
- [34] Corrosion between the Components of Modular Femoral Hip Prostheses. J. P. Collier et al.; *The Journal of Bone and Joint Surgery* (1992), Vol.74-B (4):511-517.
- [35] All-polyethylene Tibial Components Generate Higher Stress and Micromotions than Metal-backed Components than Metal-backed Tibial Components in Total Knee Arthroplasty. J. Brihault et al.; *Knee Surg. Sports Traumatol. Arthrosc.* (2016), Vol.24:2550-2559.
- [36] Manual: *Abaqus 6.12. Getting Started with Abaqus: Interactive Edition.*
- [37] [https://upload.wikimedia.org/wikipedia/commons/4/41/Abaqus\\_software\\_FEA\\_process.png](https://upload.wikimedia.org/wikipedia/commons/4/41/Abaqus_software_FEA_process.png); 30/03/2017
- [38] Validation of a Parametric Finite Element Human Femur Model. K. F. Klein et al; *Traffic Injury Prevention* (2017), Vol.18 (4):420-426.



- [39] Development of a Parametric Finite Element Model of the Proximal Femur using Statistical Shape and Density Modeling. D. P. Nicoletta et al; *Comput. Methods Biomed Engin* (2012), Vol.15 (2):101-110.
- [40] Parametric Finite Element Model of Femur from CT Data. M. Armand et al.; *SB XXth Congress - ASB 29th Annual Meeting* (2005).
- [41] <http://orthoinfo.aaos.org/topic.cfm?topic=a00377>. J. R. H. Foran; *American Academy of Orthopaedic Surgeons* (2015)
- [42] <http://www.ortopediaweb.net/web/la-displasia-congenita-dellanca/5/>; 30/03/2017
- [43] <http://www.surreyorthopaedicclinic.com/procedures/hip/>; 30/03/2017
- [44] Changes in Trabecular Pattern of the Upper end of the Femur as an Index of Osteoporosis. M. Singh; *J. Bone Joint Surg.* (1970), Vol.52:457-467.
- [45] <http://www.deviceinnovation.com/index.php?lay=show&ac=article&Id=284909>;  
30/03/2017
- [46] [http://www.kosinmedicalsupply.com/LINK\\_page01.htm](http://www.kosinmedicalsupply.com/LINK_page01.htm); 30/03/2017